NEOs in the thermal infrared (NEATM, TPM) &
Pre-impact detectability of a Chelyabinsk-type object

Thomas Müller, MPI für Extraterrestrische Physik, Garching, Germany (tmueller@mpe.mpg.de)

https://www.youtube.com/watch?v=iCawTYPtehk
Credit: Aleksandr Ivanov

Why Infrared?

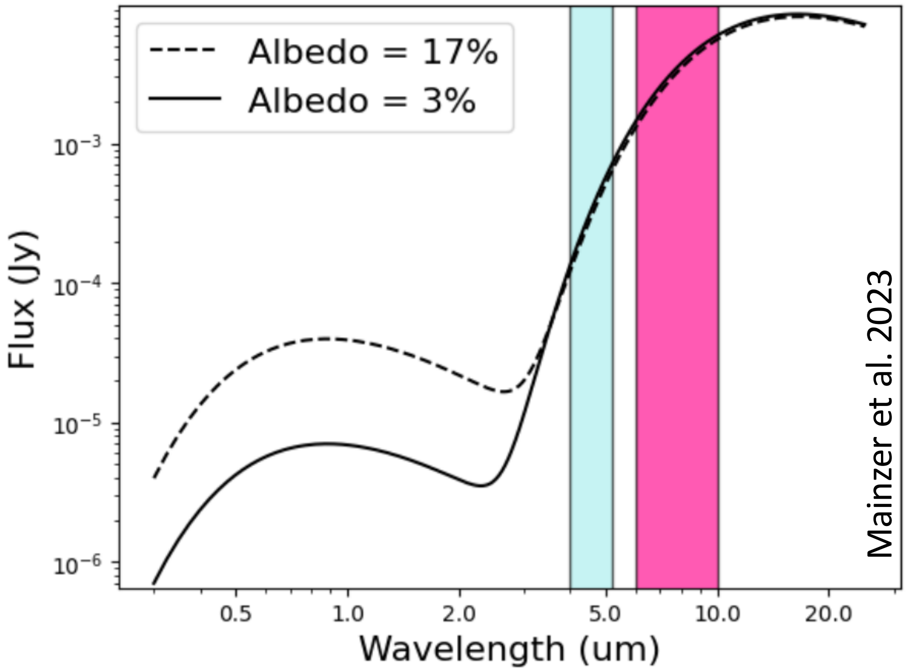

- About 90% of the incoming solar radiation is emitted in the IR
- The risk of source confusion (stars, galaxies) is in the mid-IR about 2 orders of magnitude lower then at visible λ
- The **high IR-VIS flux ratio** and the **reduced confusion risk** are especially advantageous for observing NEOs which are often viewed at large phase angles and close to the Sun.
- Visible observations of irregularly-shaped NEOs at high phase angle also suffer from rotational variations of the small, illuminated surface areas

- In contrast, thermal IR observations present a different scenario: small, fast-rotating NEOs exhibit **nearly isothermal surfaces** with temperatures ranging from 300 to 400 K. Consequently, the likelihood of early detection is enhanced at IR wavelengths, especially at large phase angles.
- Additionally, IR measurements provide **valuable constraints on an object's size, albedo, and thermal characteristics** indicative for the surface material strengths

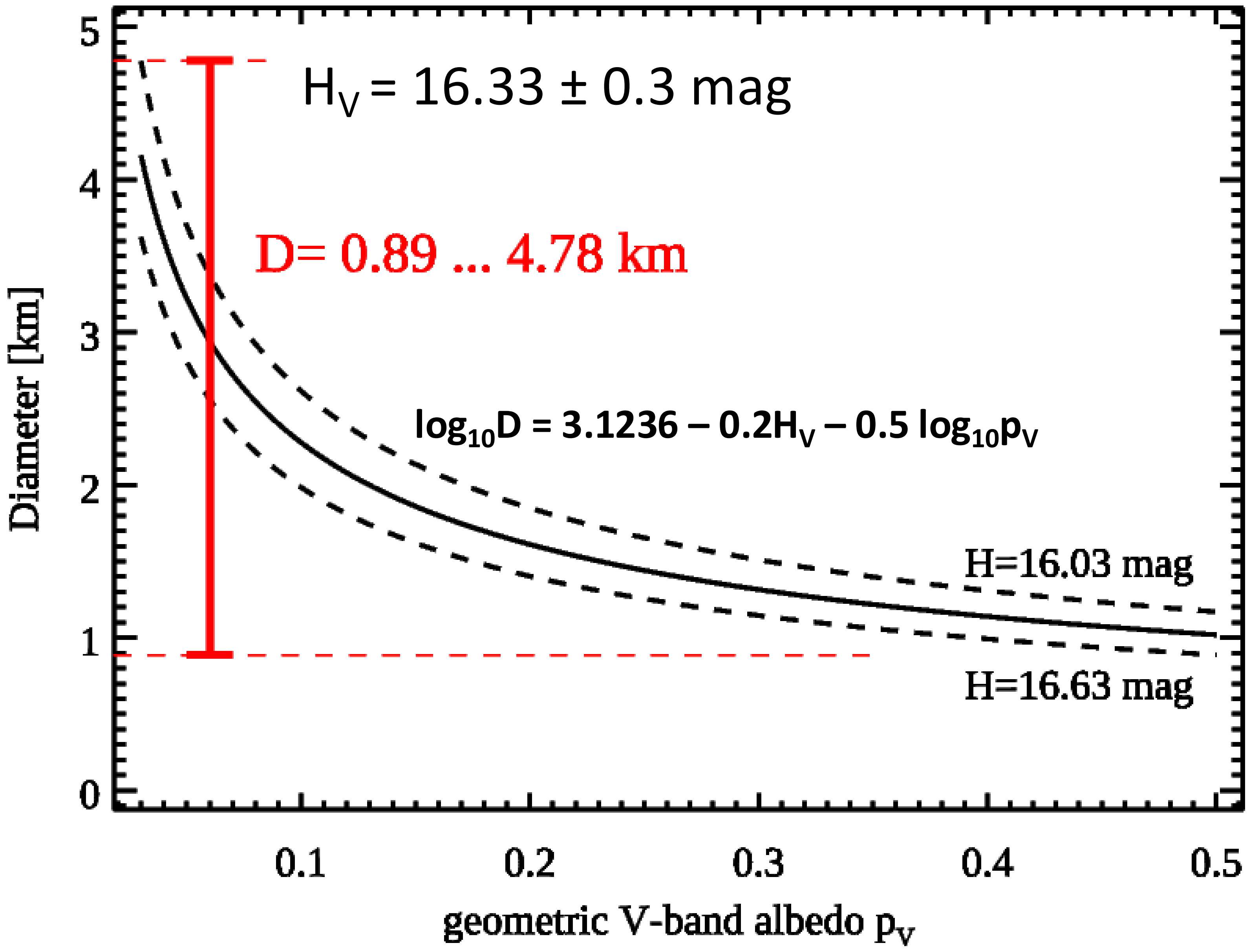

$H_V = 16.33 \pm 0.3$ mag
D= 0.89 ... 4.78 km
$\log_{10}D = 3.1236 - 0.2H_V - 0.5 \log_{10}p_V$
H=16.03 mag
H=16.63 mag
Diameter [km]
geometric V-band albedo p_V
0
1
2
3
4
5
0.1
0.2
0.3
0.4
0.5

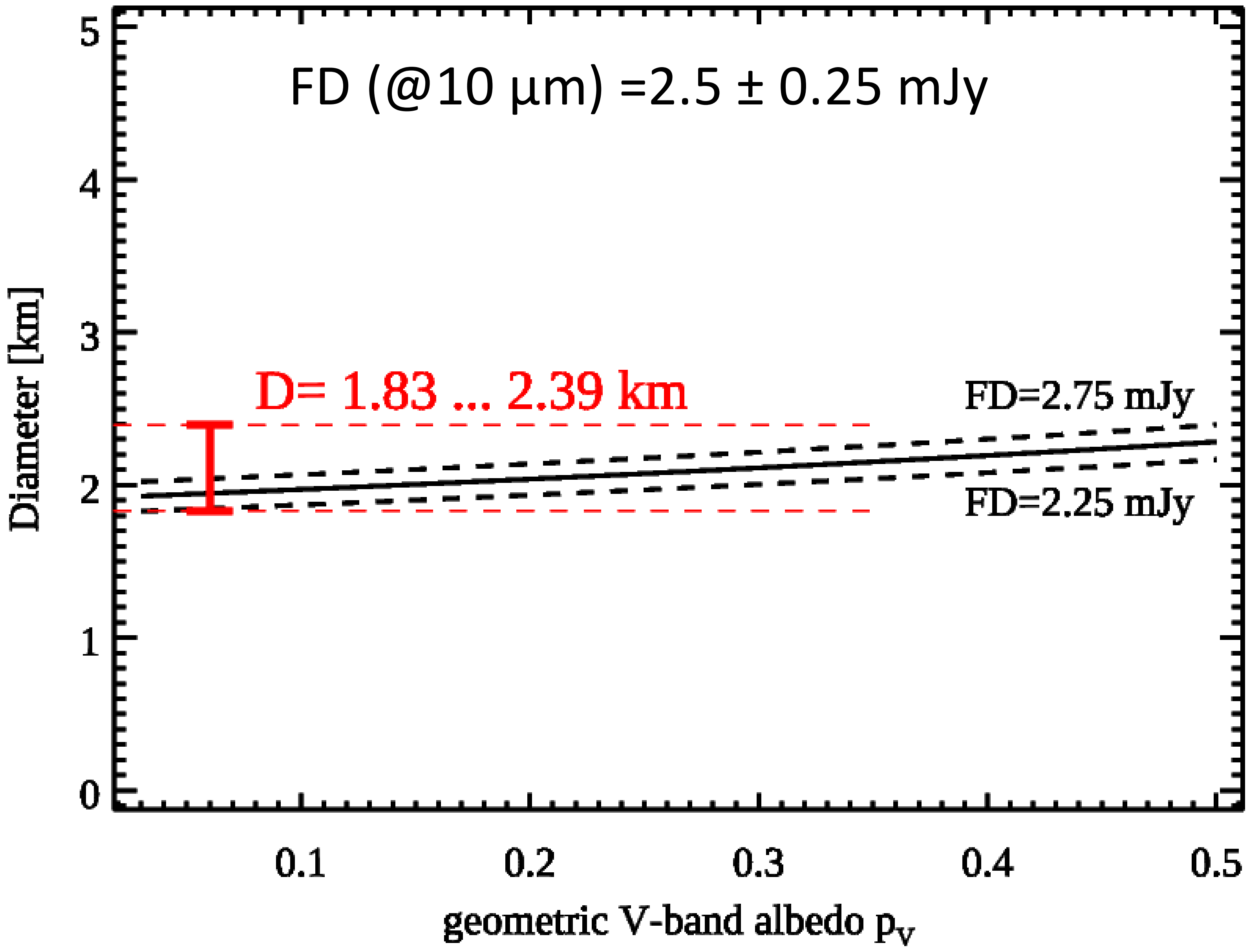

FD (@10 µm) =2.5 ± 0.25 mJy
D= 1.83 ... 2.39 km
FD=2.75 mJy
FD=2.25 mJy
Diameter [km]
geometric V-band albedo p_V
0
1
2
3
4
5
0.1
0.2
0.3
0.4
0.5

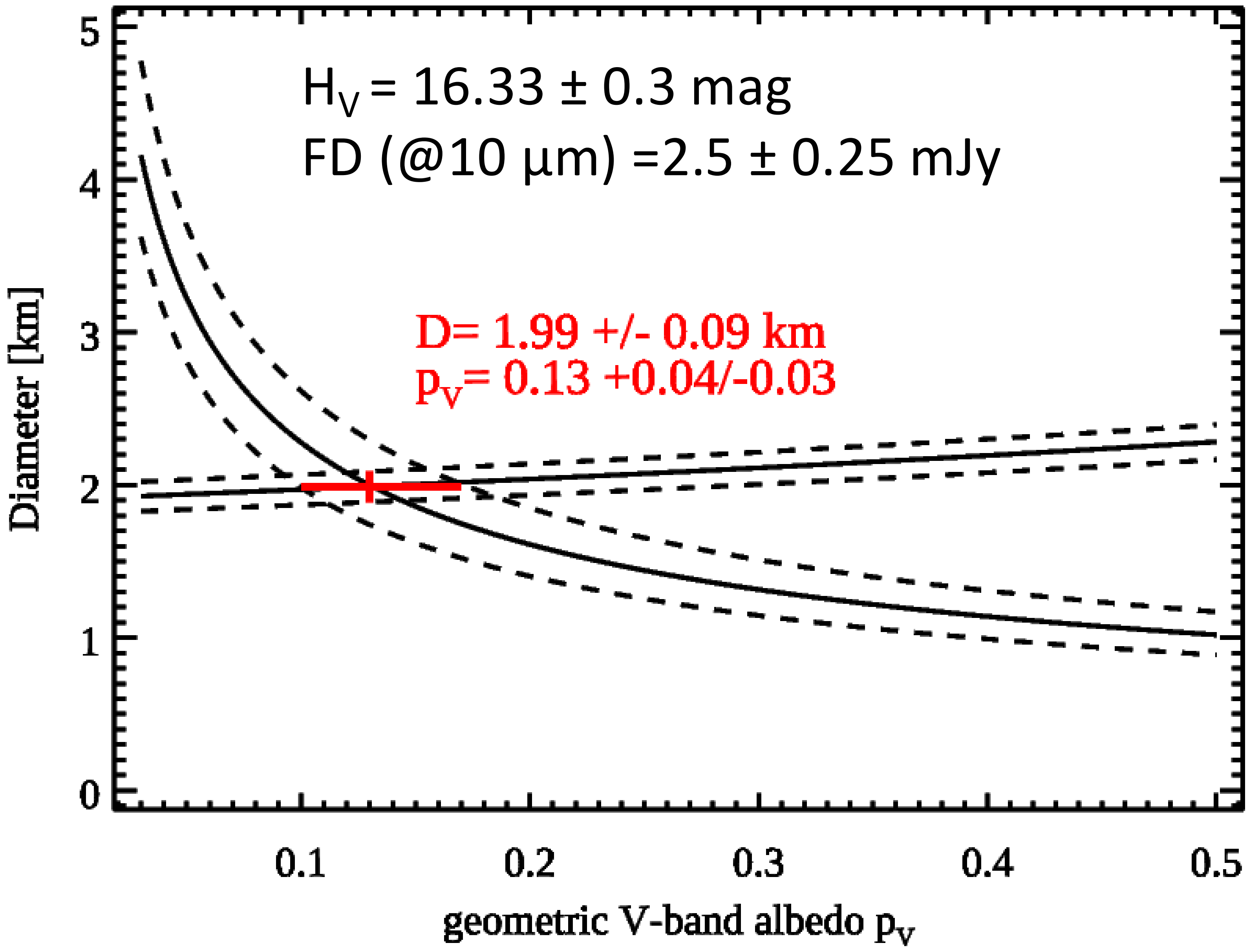

HV = 16.33 ± 0.3 mag
FD (@10 µm) =2.5 ± 0.25 mJy
D= 1.99 +/- 0.09 km
pV= 0.13 +0.04/-0.03
Diameter [km]
geometric V-band albedo pV
0
1
2
3
4
5
0.1
0.2
0.3
0.4
0.5

Size determination for MBAs (larger objects, limited phase angle range):

- H-mag only: factor 4-5 uncertainty in size
- IR detection, no H-mag: ±20-30% via NEATM
- IR detection, with H-mag: ±10-20% via NEATM
- Multiple/multi-band detections of objects with known orbit and H-mag: ±10% via TPM techniques (if spin-shape solution available: ±5%)

Size determination for NEAs (small, fast(er) rotation, shape, large phase angles):

→ **NEA radiometric size determination easily possible (WISE, NEO Surveyor, NEOMIR, …), but**

  - Lower quality due to large changes in cross section (shape, aspect angle)
  - No thermal model validation for objects at large (>90°) phase angles
  - Unknown surface roughness and thermal inertia effects (bare rock, porous rocks, fine/coarse grain regolith on low-g surface)
  - Unknown temperature distribution for small, fast-rotating asteroids
  - Thermal properties change for highly eccentric orbits

NEATM (Harris 1998) application: Ryugu

- Assuming a spherical shape model and only day-side emission is considered (using the absolute phase angle $|\alpha|$)
- $T = [S\,(1 - A)\,\cos(\Theta)/(\eta\,\varepsilon\,\sigma)]^{1/4}$ where A is the Bond albedo, ε is the bolometric emissivity (assumed to be 0.9), σ is the Stefan- Boltzmann constant, S is the solar insolation at the distance of the object, Θ is the angle away from the sub-solar point, and η is the beaming parameter.
- The reflected sunlight (at zero phase angle) is determined by the visible geometric albedo p_V. It is connected to the Bond albedo A through the phase integral q, as $A = q\,p_V$
- *q* can be calculated from the slope parameter *G* via $q = 0.290 + 0.684\,G$ (Bowell et al. 1989)

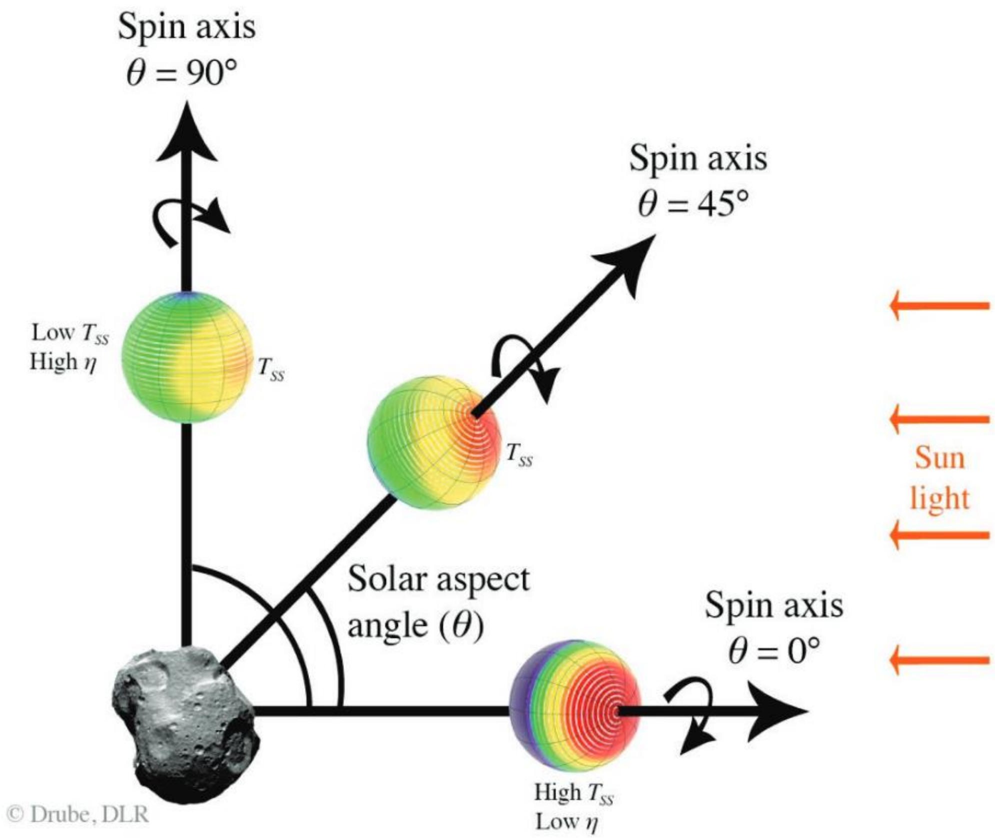

Application to all available remote observations from Spitzer-IRAC (ch1,ch2)/-IRS, WISE-W1/-W2, Subaru-COMICS, AKARI-IRC, Herschel-PACS

NEATM Beaming phase function

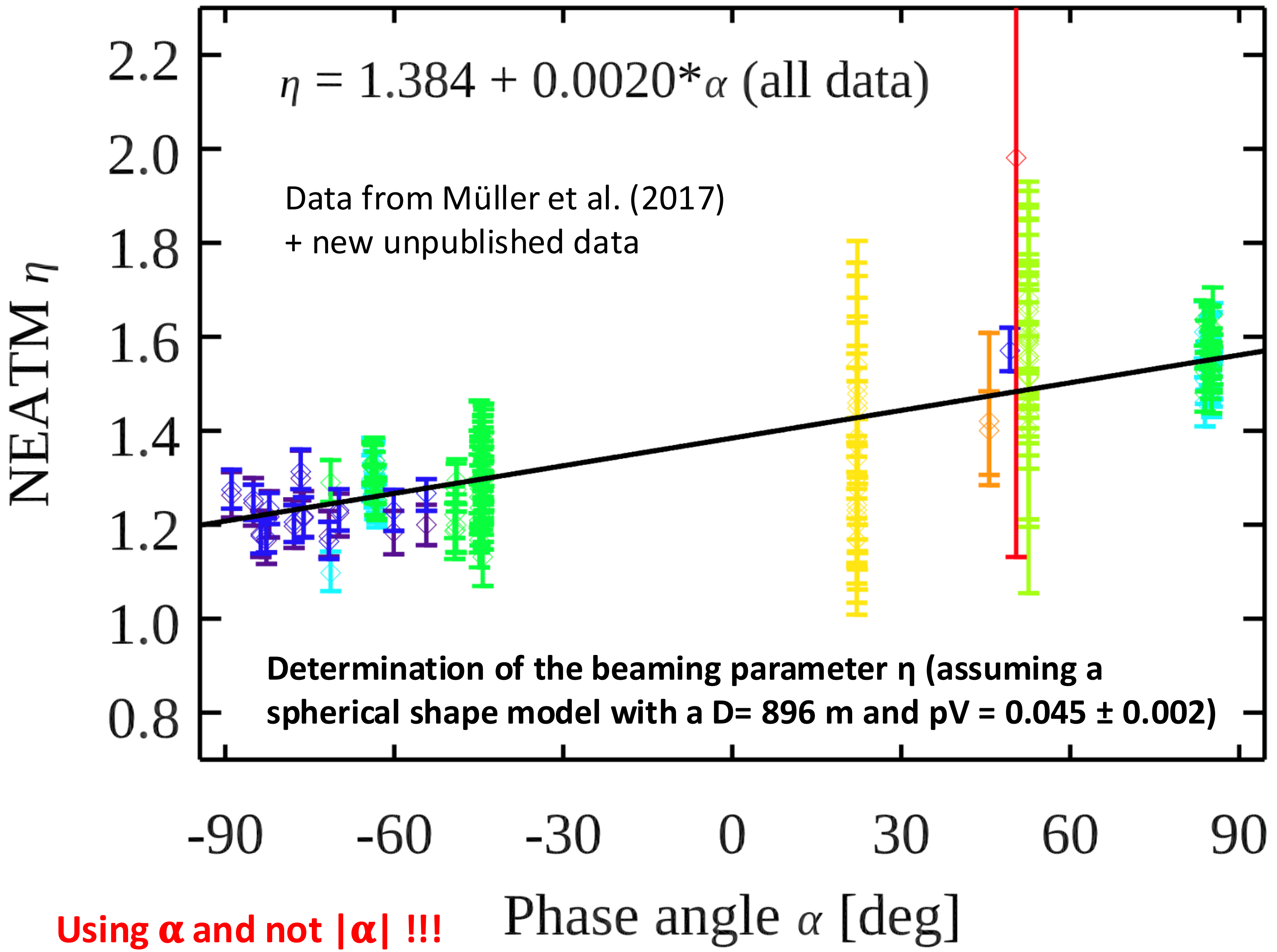

Using α and not |α| !!!

NEATM Beaming phase function

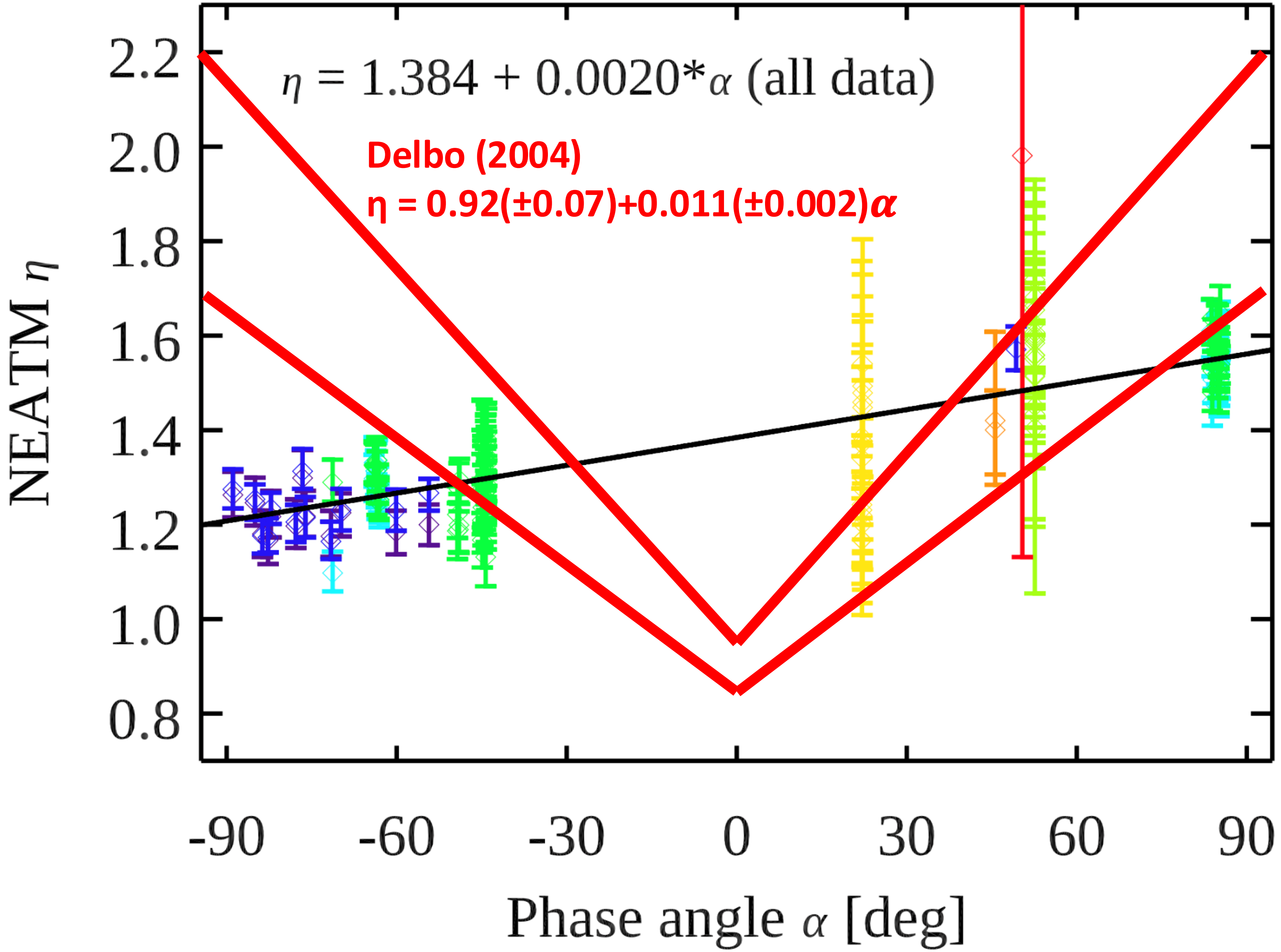

NEATM Beaming phase function

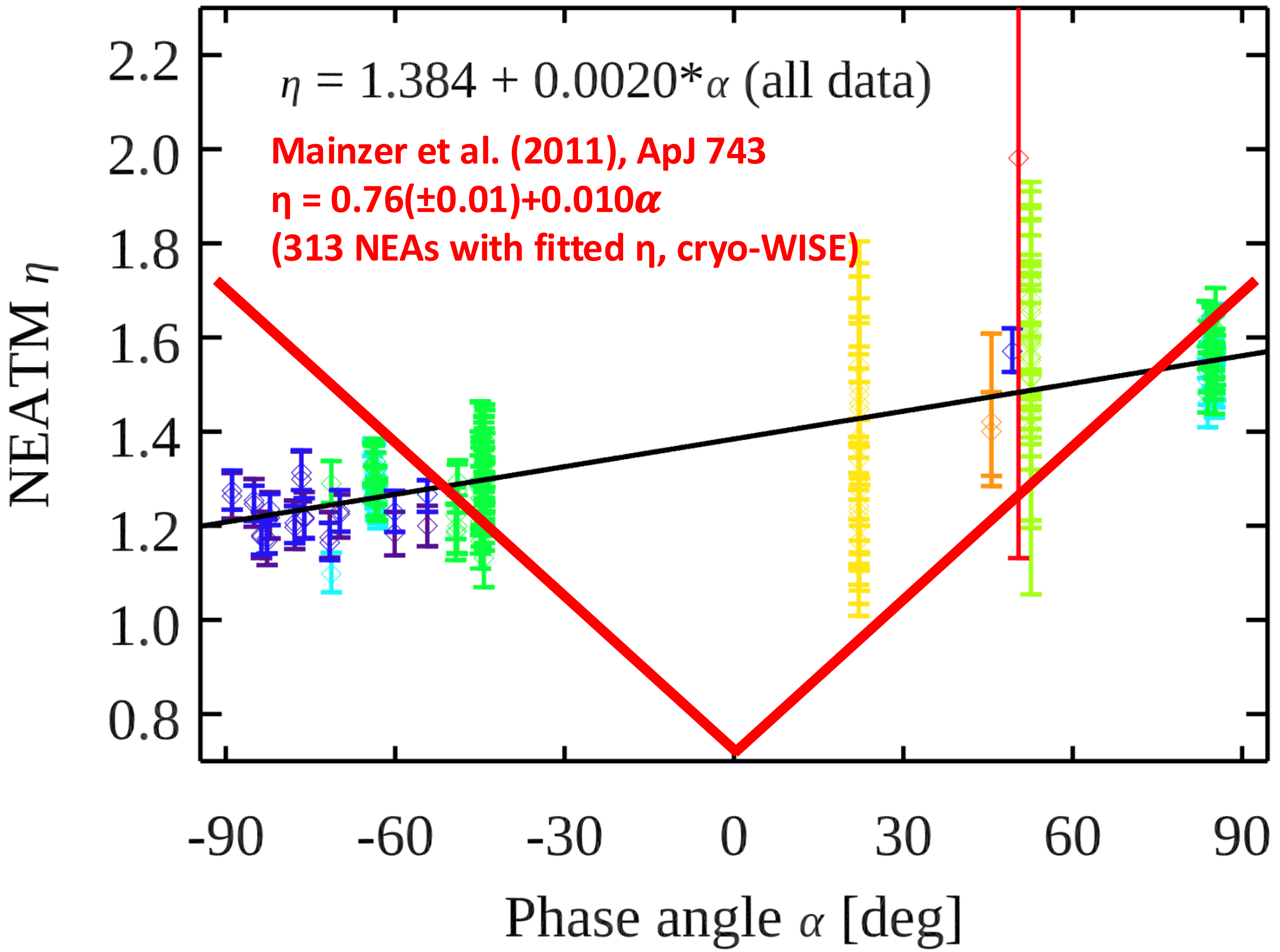

NEATM Beaming phase function

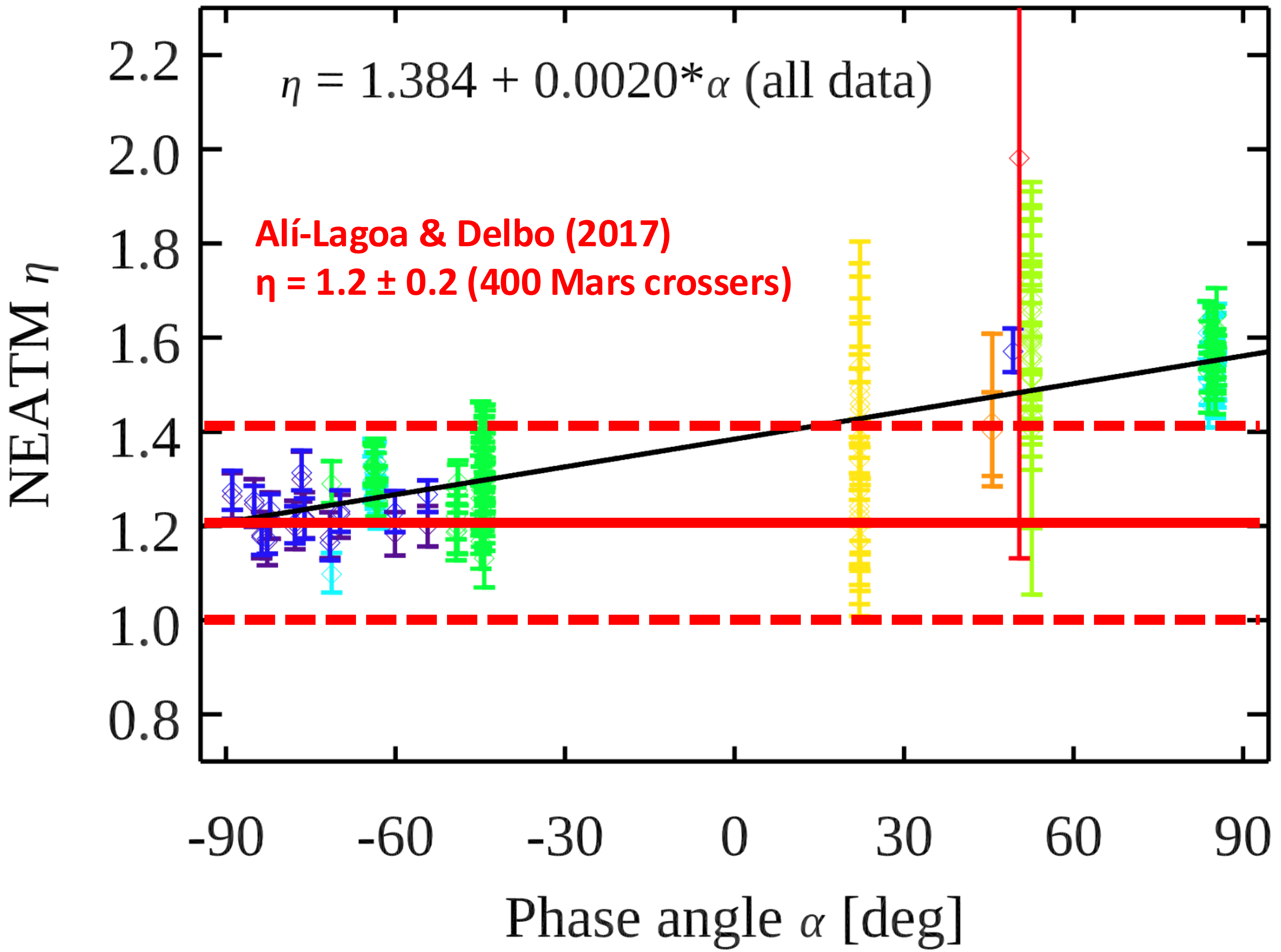

NEATM results: Ryugu

- Using NEATM with $\eta = (1.384 \pm 0.005) + (0.0020 \pm 0.0002)\alpha$ works very well and allows to reproduce Ryugu's size and albedo (**NOTE**: η calculation requires signed α!)
- This NEATM solution explains the available thermal measurements (within their absolute flux errors) over all phase angles (-90° … +90°), wavelengths (3.3 to 70 μm), rotational phases or heliocentric distances (0.98 … 1.42 au), the $\chi^2_{reduced} = 1.2$!
- The NEATM η slope is a strong indication for a retro-grade rotator
- The η slope is also indicative of a thermal inertia close to 300 tiu (assuming a rotation period of 7.6 hours and an equator-on viewing geometry)
- Published η-solutions are not working very well for Ryugu (on only for specific phase-angle ranges and wavelengths)

- **But η is not only phase-angle dependent (with the slope depending on the object's thermal and rotation properties), it also changes with wavelengths and heliocentric distance (for the same object!)**

TPM application: Ryugu

(Lagerros 1996, 1997, 1998; Müller & Lagerros 1998, 2002, all in A&A)

- A rough surface model is assumed for each patch (considering only very small segments)
- The effect of heat conduction and surface roughness of the small segment is modelled and the result scaled to the entire patch
- Each small segment of a surface patch is divided into a large number of surface elements
- The **roughness** is simulated by either considering a **hemispherical crater** on otherwise flat surface, or by assuming a **Gaussian random rough surface** (see below)
- The Sun illuminates the segment and its surface elements and moves across the sky as the asteroid revolves around its axis.
- Due to the surface roughness, some elements **shadow** other surface elements which is taken into account
- Each element is heated by the Sun and by visual **light scattered** from neighbouring elements.
- Heat is exchanged with the interior through heat conduction, assuming the elements to be 1-D slabs isolated from neighbouring surface elements
- For temperature calculations the bolometric emissivity ε_{bolo} is relevant (integral of the spectral emissivity weighted by the solar spectrum)
- The (disk-integrated) flux (or emittance) is calculated by integrating over all temperatures and by considering the hemispherical spectral emissivity ε_{spec} at a given wavelengths (depends on T^4!)

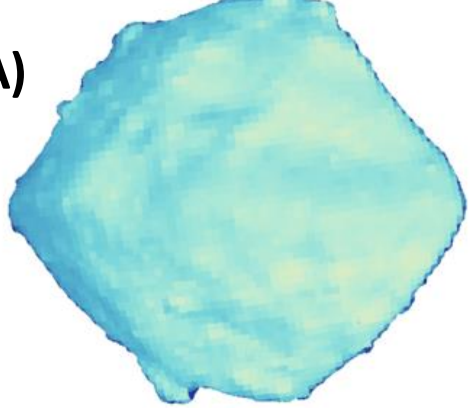

Hyb2_tir_20181114_073228_l3:
r=1.335 au, Δ=19.23 km, α = -4.8°,
$(\lambda,\beta)_{SubSC}$ = (356.4,-1.3),
$(\lambda,\beta)_{SubSolar}$ = (351.6,-1.9)

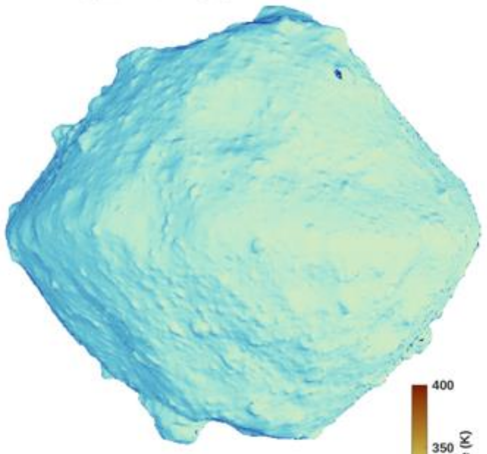

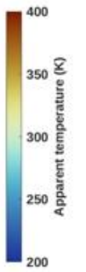

TPM with Γ=350 tiu,
rms = 45° (sph crater),
ε =0.98, SPC_200k

TPM roughness effects f(α)

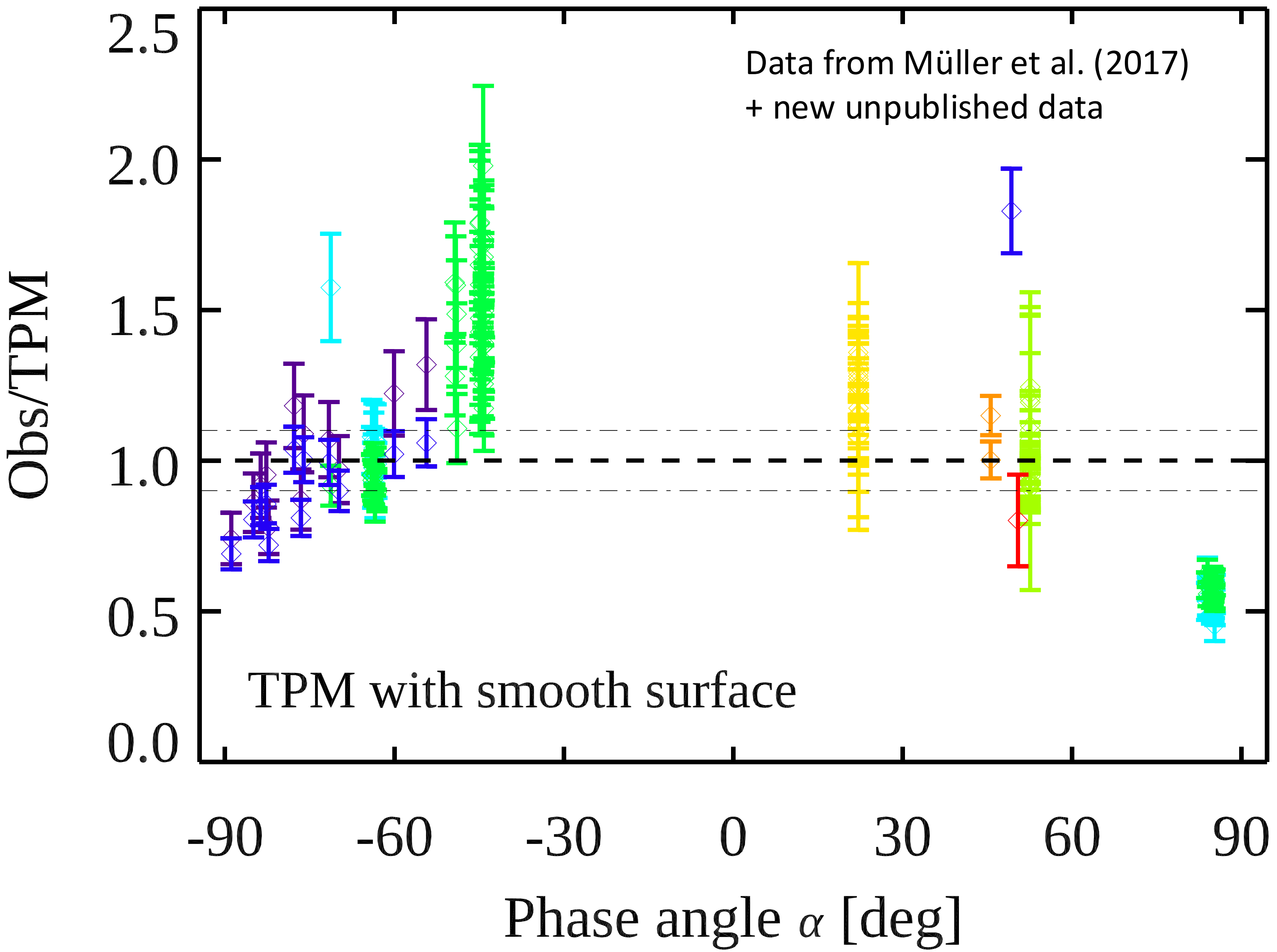

Using the high-resolution shape model and the published thermal inertia for Ryugu

TPM roughness effects f(α)

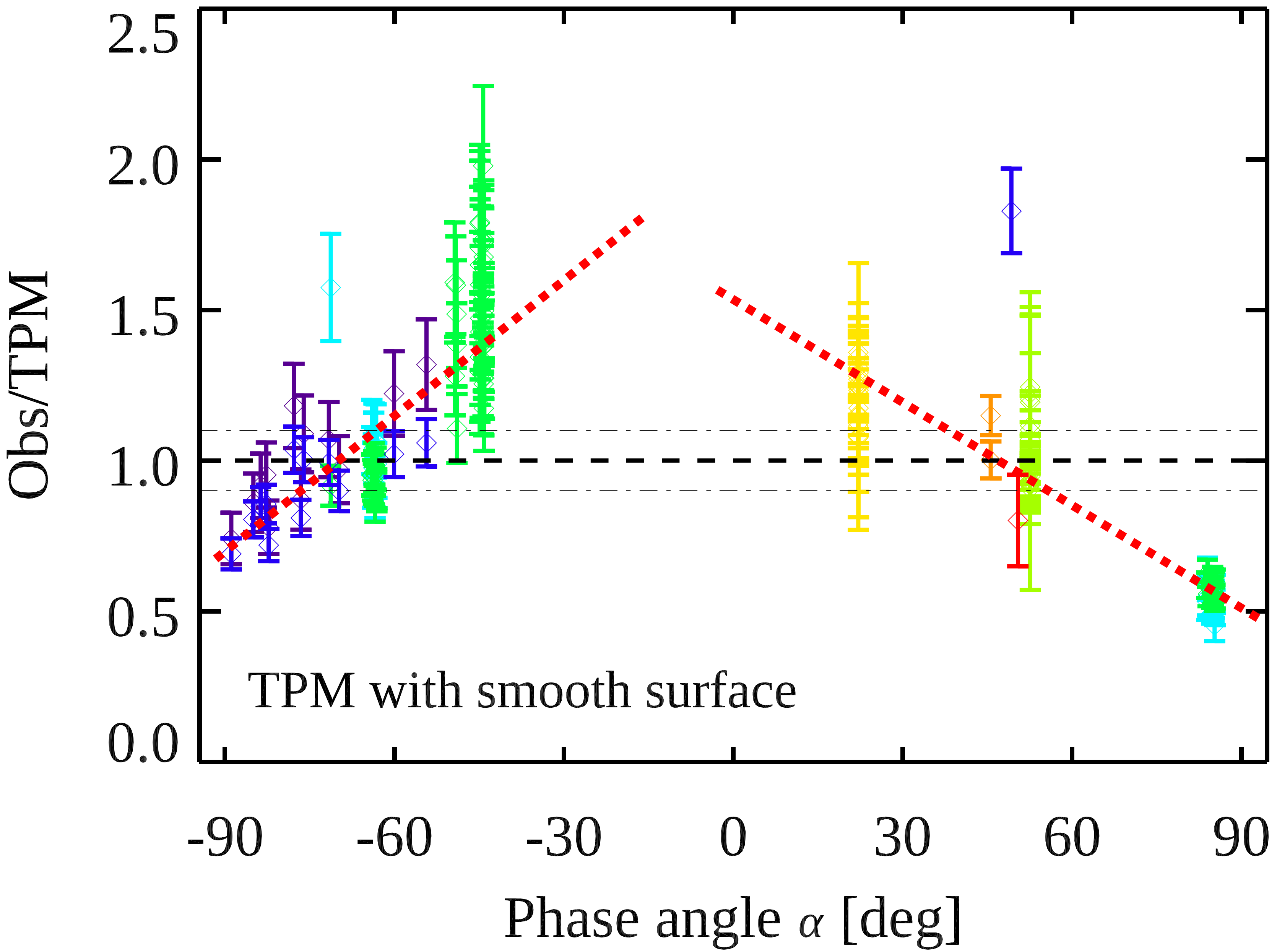

Using the high-resolution shape model and the published thermal inertia for Ryugu

TPM roughness effects f(λ)

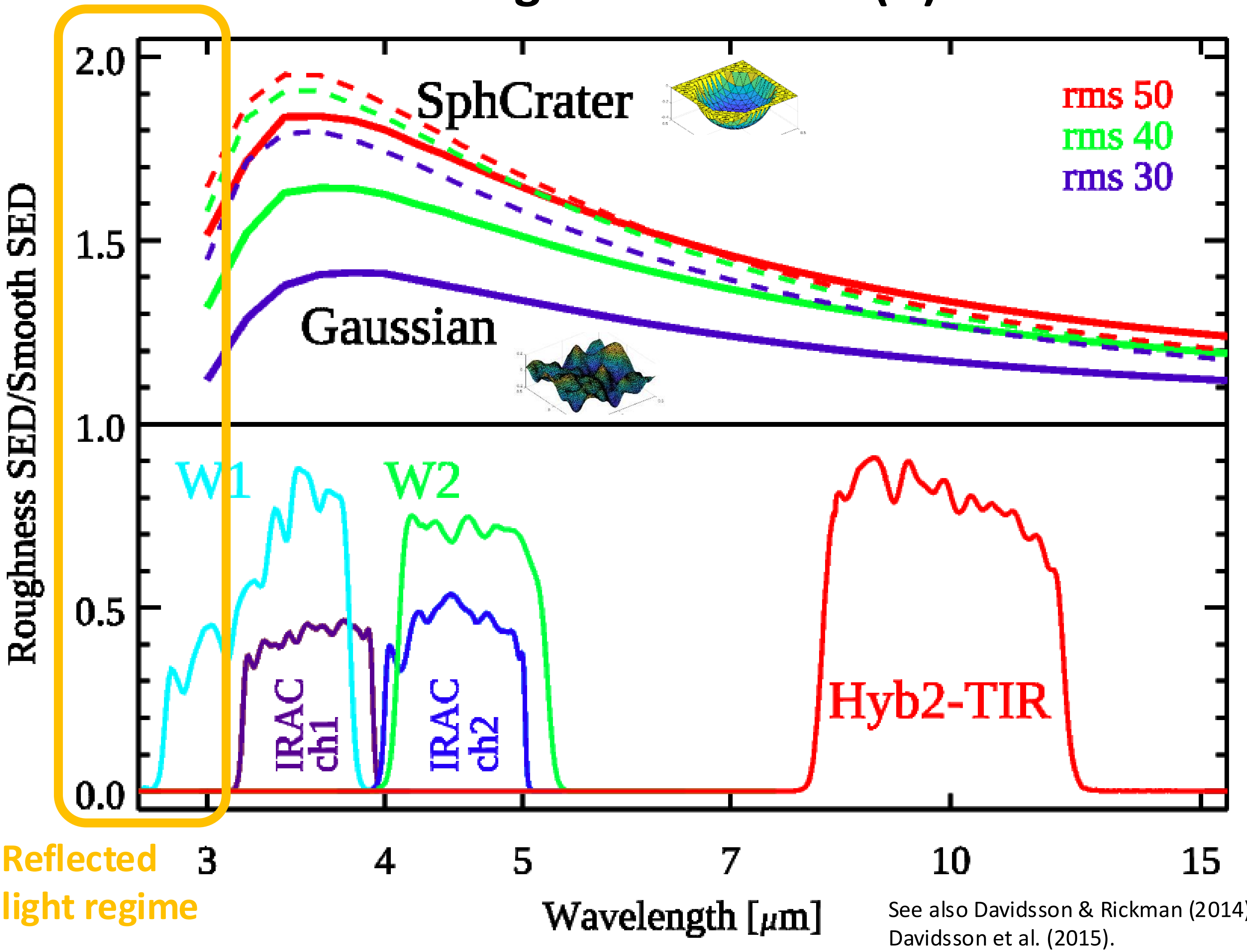

See also Davidsson & Rickman (2014); Davidsson et al. (2015).

Using the asteroid thermophysical model code by Lagerros (1996, 1997, 1998)
Müller & Lagerros (1998, 2002, all in A&A), no surface roughness added

TIR image from Okada+20

TPM prediction (Γ=225)

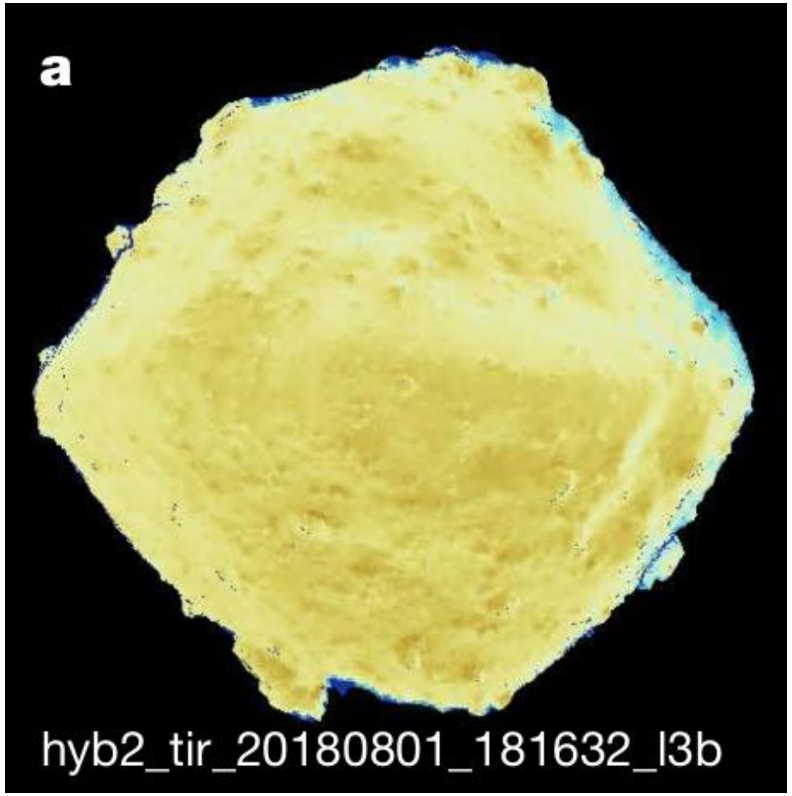

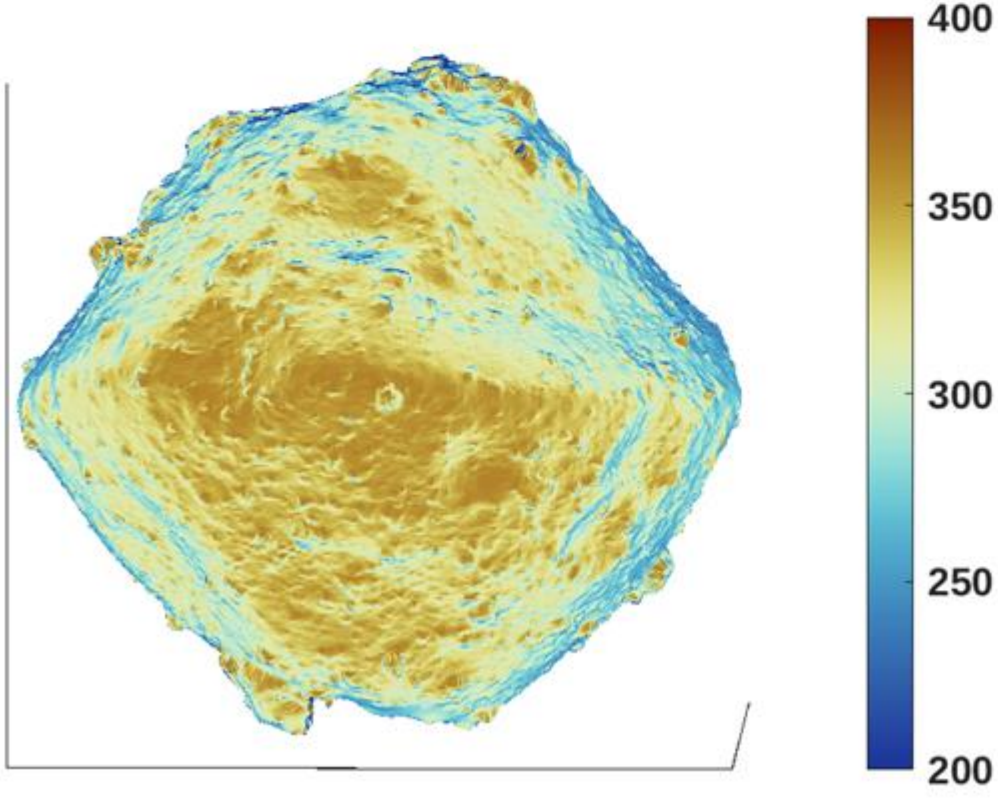

TPM roughness effects

Using the asteroid thermophysical model code by Lagerros (1996, 1997, 1998) Müller & Lagerros (1998, 2002, all in A&A), adding surface roughness (hemispherical craters on otherwise flat surface)

TIR image from Okada+20

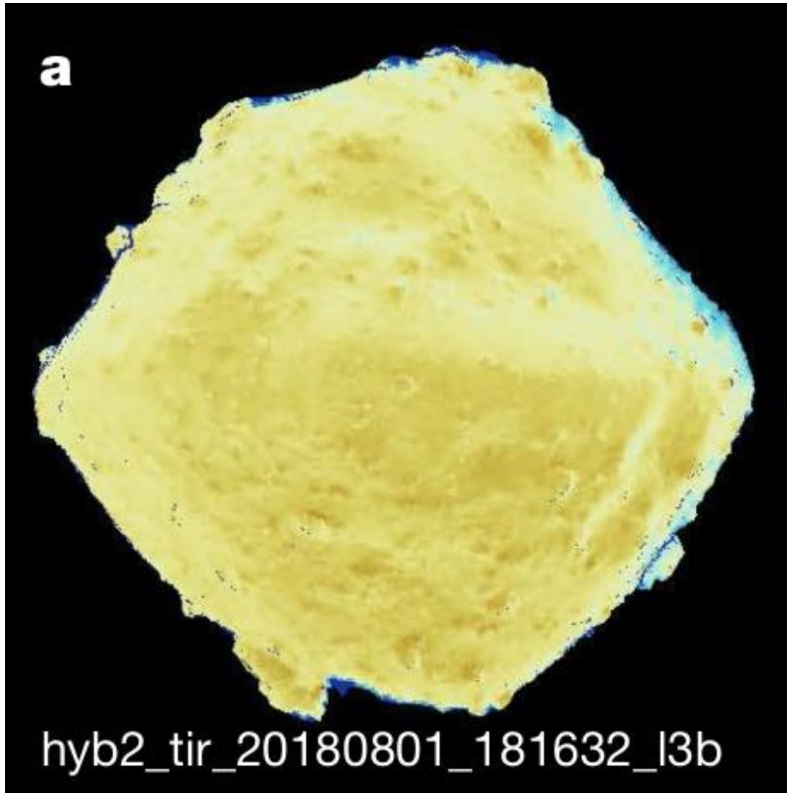

TPM prediction (Γ=225, rms 47°)

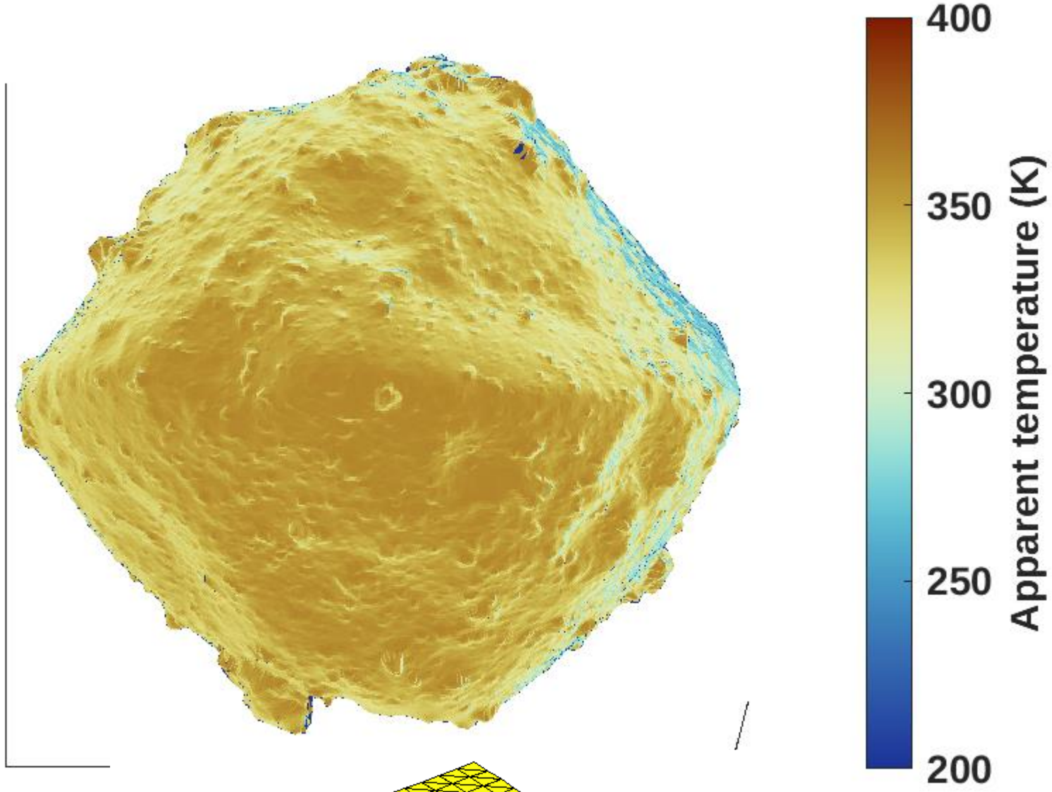

TPM roughness effects

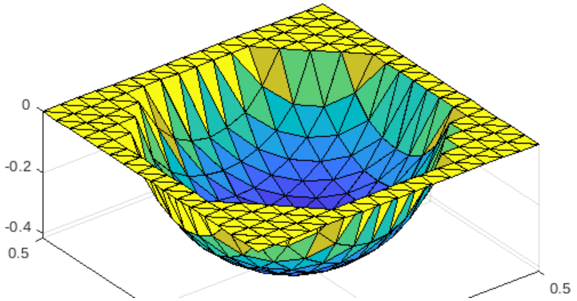

Using the asteroid thermophysical model code by Lagerros (1996, 1997, 1998) Müller & Lagerros (1998, 2002, all in A&A), adding surface roughness (assuming Gaussian random rough surface)

TIR image from Okada+20

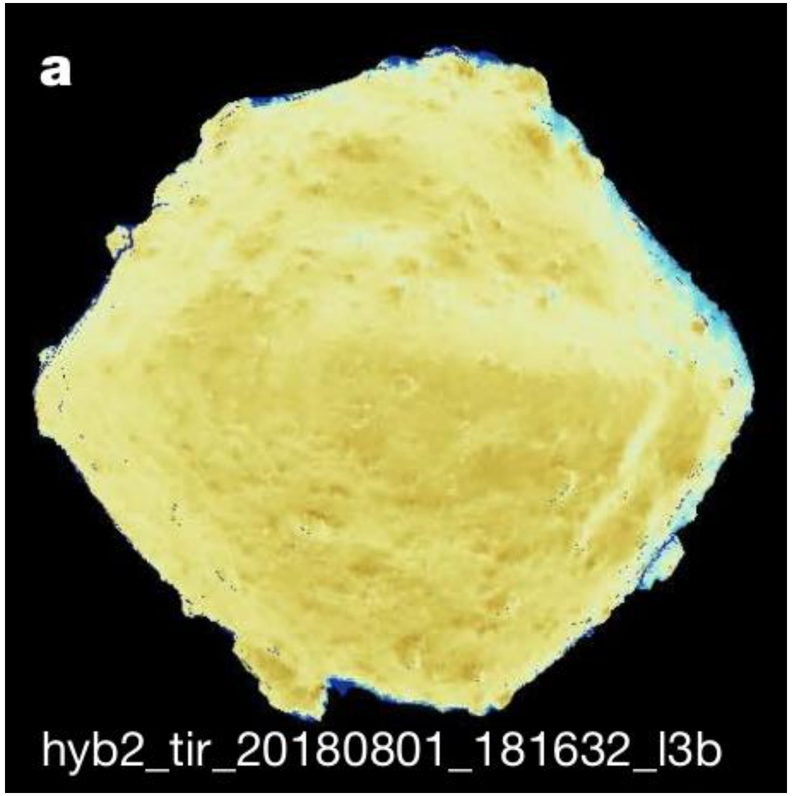

TPM prediction (Γ=225, rms 40°)

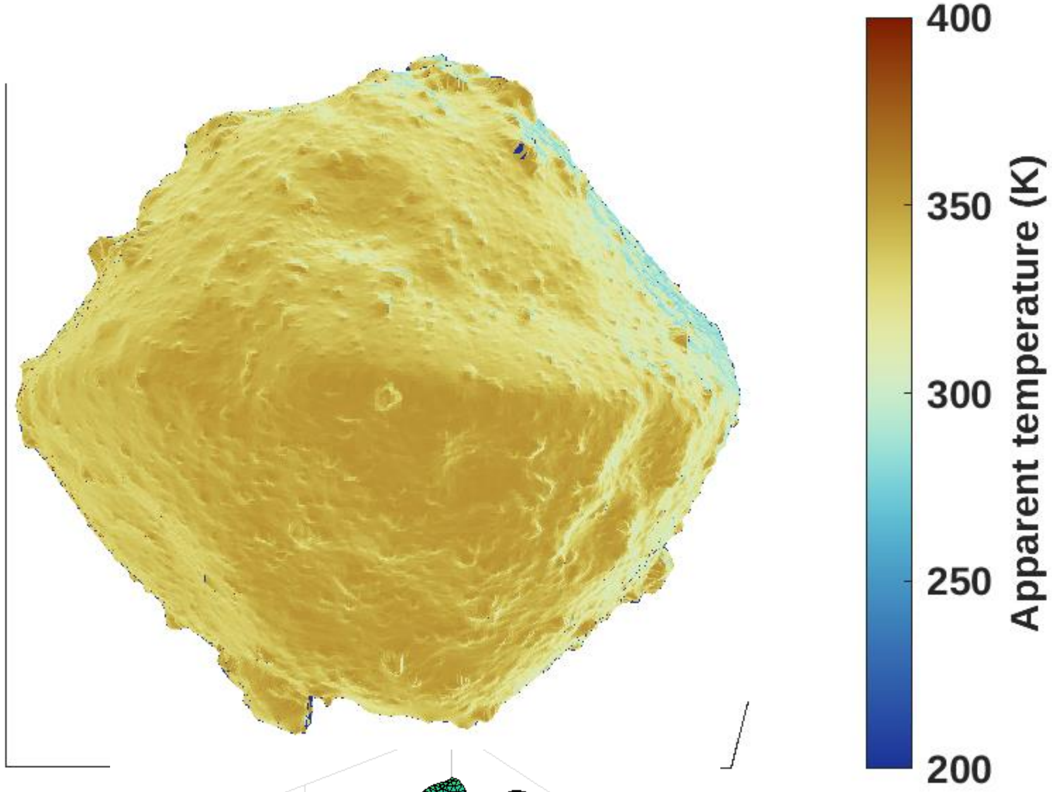

TPM roughness effects

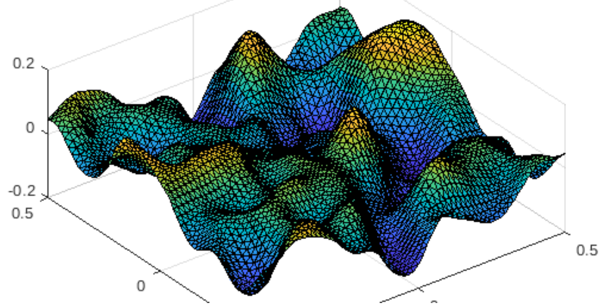

TPM results: Ryugu

- TPM solution (ε_{bolo} ~0.98, TI = 300-400 tiu, roughness: 30-50° rms of surface slopes) **explains the remote data** very well, including before/after opposition effects, short-wavelength data, thermal lightcurves, amplitudes, absolute fluxes, … AND allows to **explains the surface temperature distribution** (TIR images) in a qualitative way
- Roughness modeling (hemispherical craters or Gaussian random surfaces) is crucial, but results, for exactly the same rms of surface slopes, are not identical
- Thermal inertia as a function of temperature (or r_{helio}) is noticeable for Ryugu in-situ data

Chelyabinsk progenitor (ChPG) orbit
(study in the context of NEOMIR project)

- Based on Popova et al. (2013): *"Chelyabinsk Airburst, Damage Assessment, Meteorite Recovery, and Characterization"*, Science 342, 6162
- Orbital elements: a=1.76 (±0.16) au, e=0.581 (±0.018), i=4.93°(±0.48°), q=0.739 (±0.020) au, T_p=2012-12-31.9 (±2.0); Impact: 2013-02-15 03:20 UTC
- 20-m size assumption (→ H=27.4/26.2/25.7 mag for p_V=0.05/0.15/0.25)

Questions:

- What's the best place to observe (L1,L2,L4,L5, Earth)? → **L1**
- Which wavelengths and why? → **mid IR (8-12 μm) produces highes SNR**
- Is the background a problem? → **yes, certainly at solar elongations <60°**
- Is the high apparent motion a problem? → **yes, in the days before Earth encounter**
- What's needed to detect (SNR >5) the ChPG as early as possible? → **close Sun-proximity observations (down to solar elongation of about 20°); fast detector readout (to avoid saturation) and synthetic tracking techniques (to take advantage of full array-crossing times)**
- Where are the problems in the SNR estimates? → **NEA model calculations**

Which is the best place to observe? → L1

Solar elongations (from L1):
- Mercury: up to 27.7°
- Venus: up to 47.0°
- Earth: 180° (±0.2°)
- Moon: 164°…180°

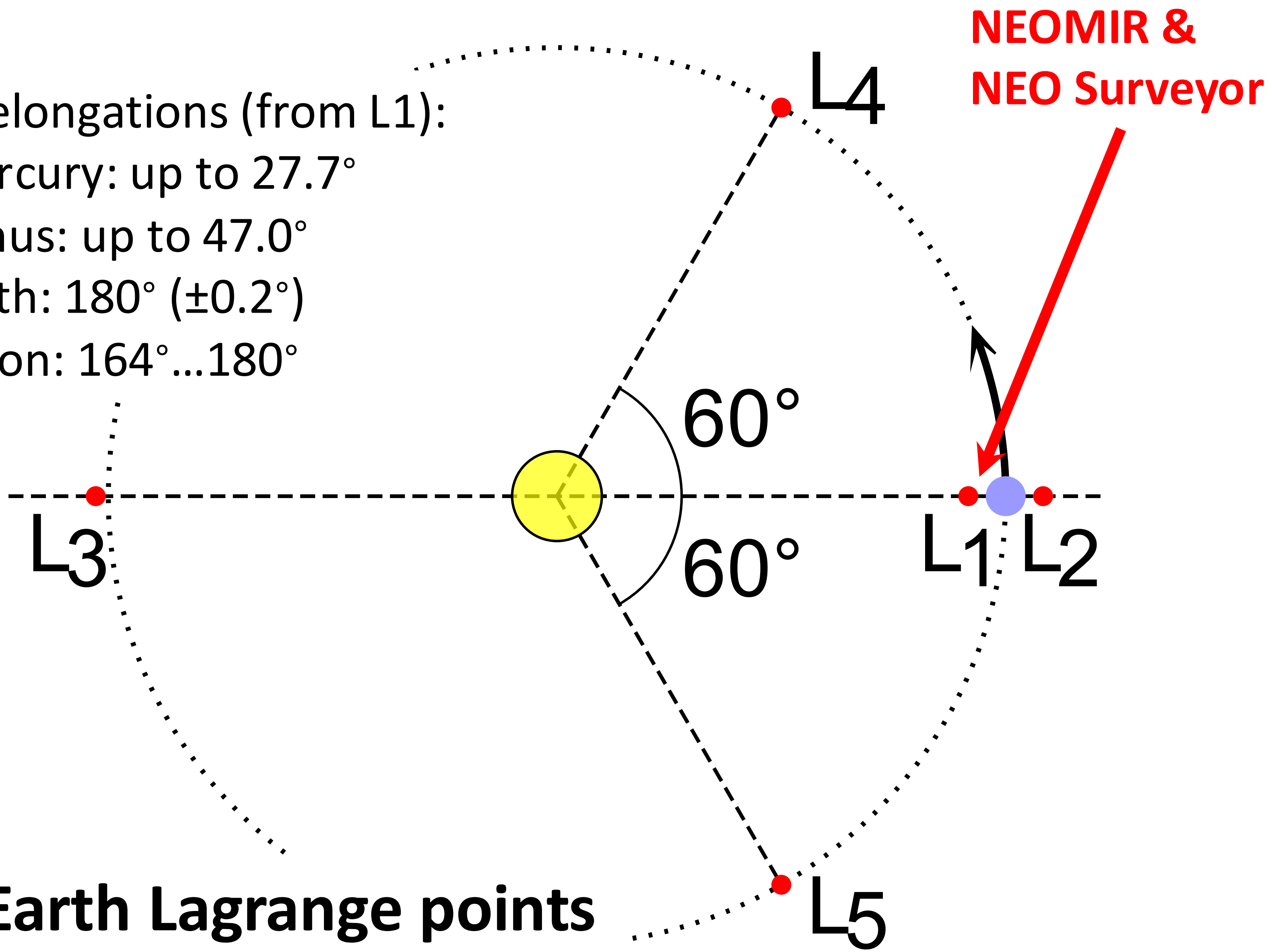

Sun-Earth Lagrange points

Chelyabinsk-progenitor (ChPG) orbit before impact

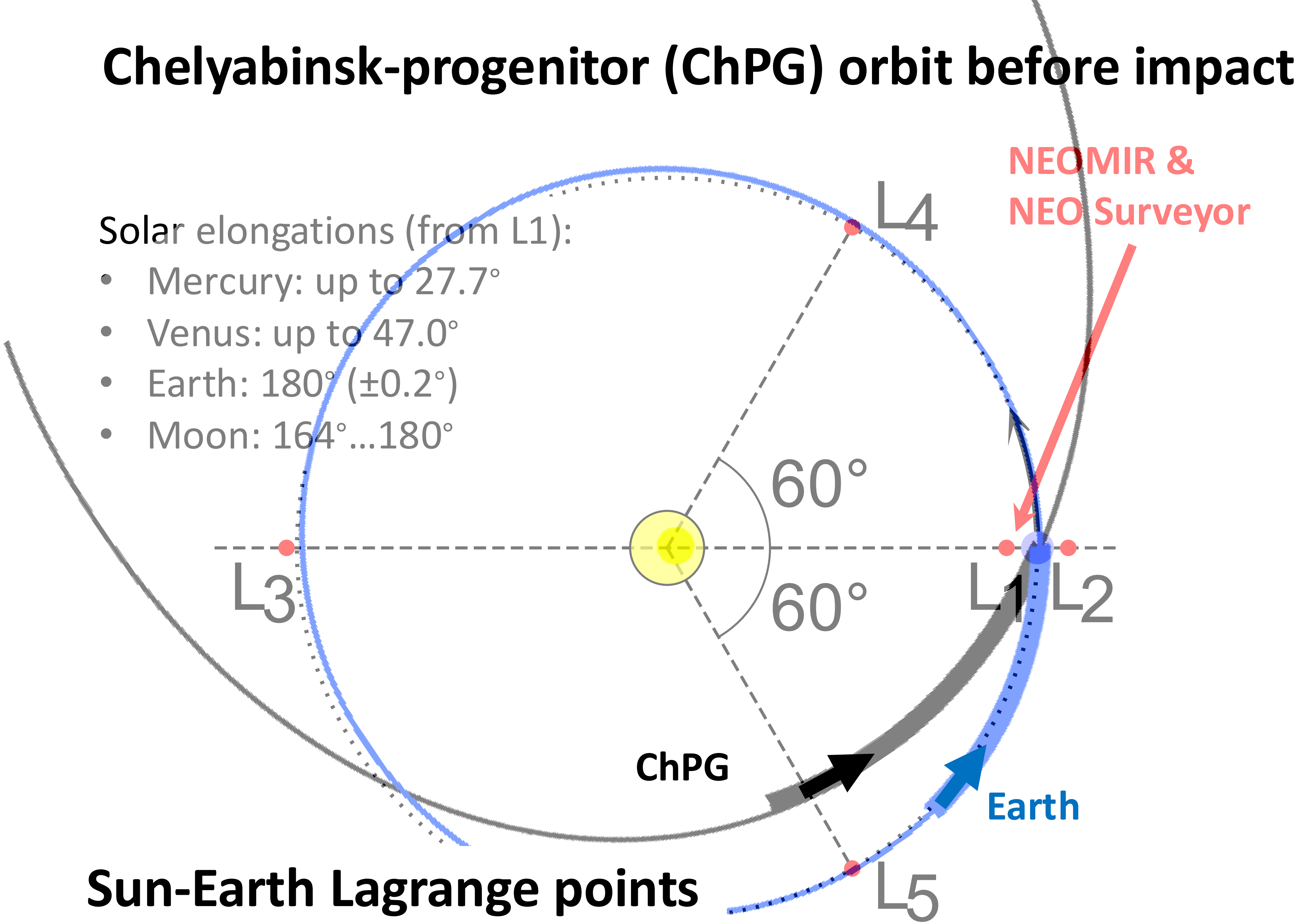

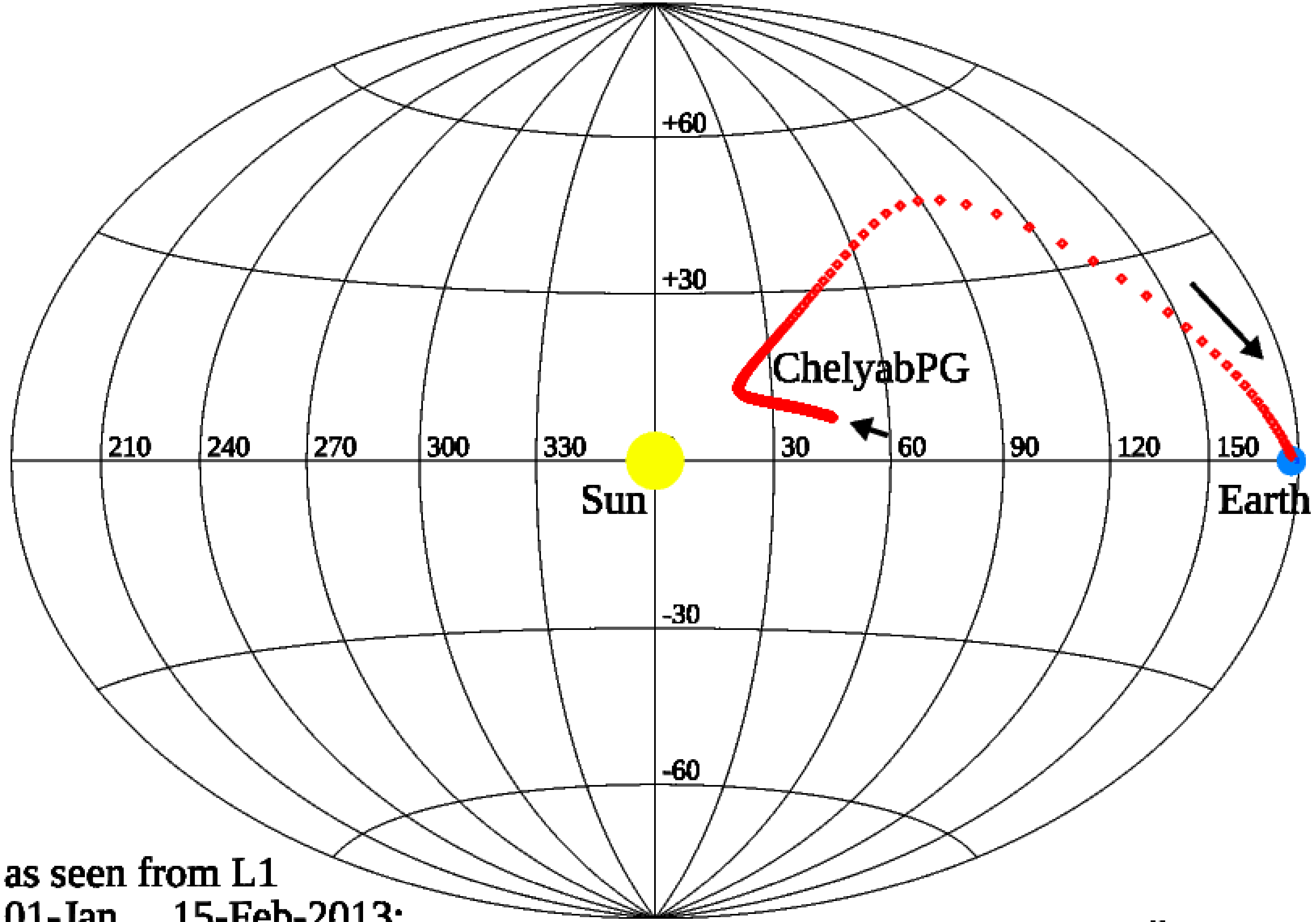

as seen from L1
01-Jan ... 15-Feb-2013:
1-h time resolution

Aitoff Projection
T.Mueller, Aug 24

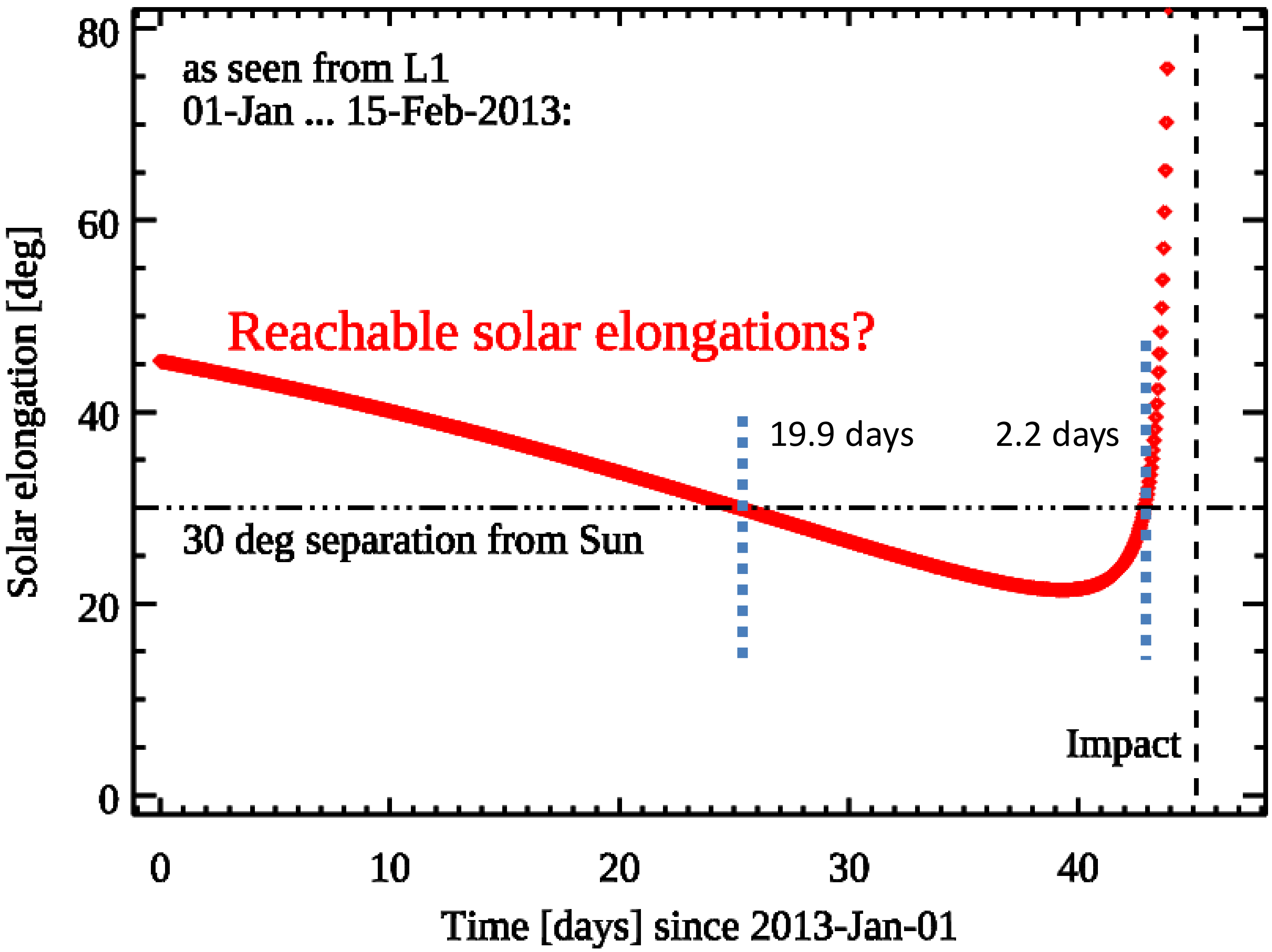

as seen from L1
01-Jan ... 15-Feb-2013:
Reachable solar elongations?
19.9 days
2.2 days
30 deg separation from Sun
Impact
Solar elongation [deg]
0
20
40
60
80
0
10
20
30
40
Time [days] since 2013-Jan-01

Is the IR background a problem? → Yes

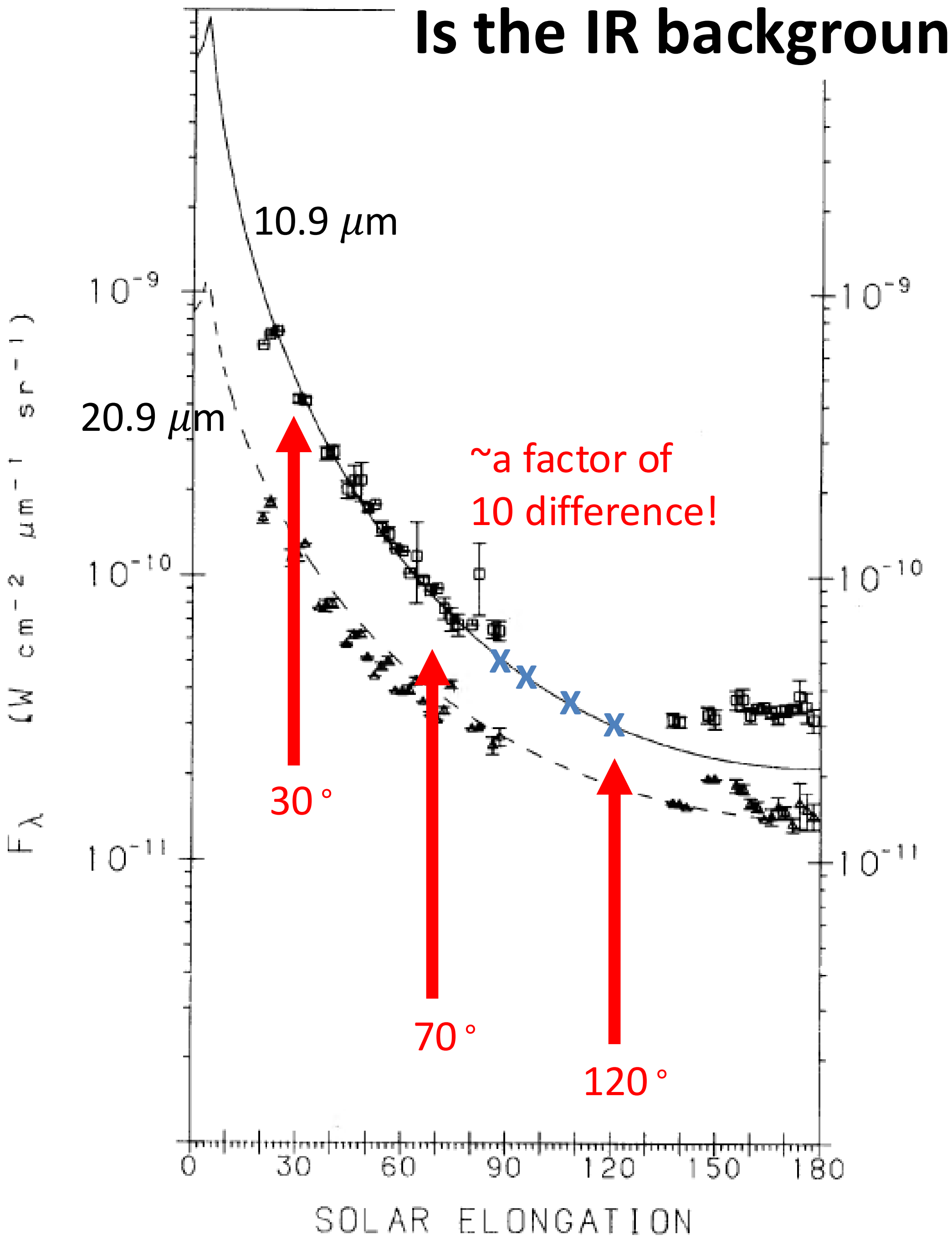

Murdock & Price (1985), rocket experiment, Fig. 12: F_{λ} as a function of solar elongation angle at 10.9 μm (squares) and 20.9 μm (triangles) in ecliptic plane.

Values from the JWST ETC at 10 μm in the ecliptic plane:

$(\lambda - \lambda_{Sun})_{ecl}$	SurfBrightness
85 °.	40 MJy/sr
90 °.	37 MJy/sr
100 °.	31 MJy/sr
120 °.	25 MJy/sr

Another tool available at:
https://irsa.ipac.Caltech.edu/applications/BackgroundModel

IR Background along apparent trajectory

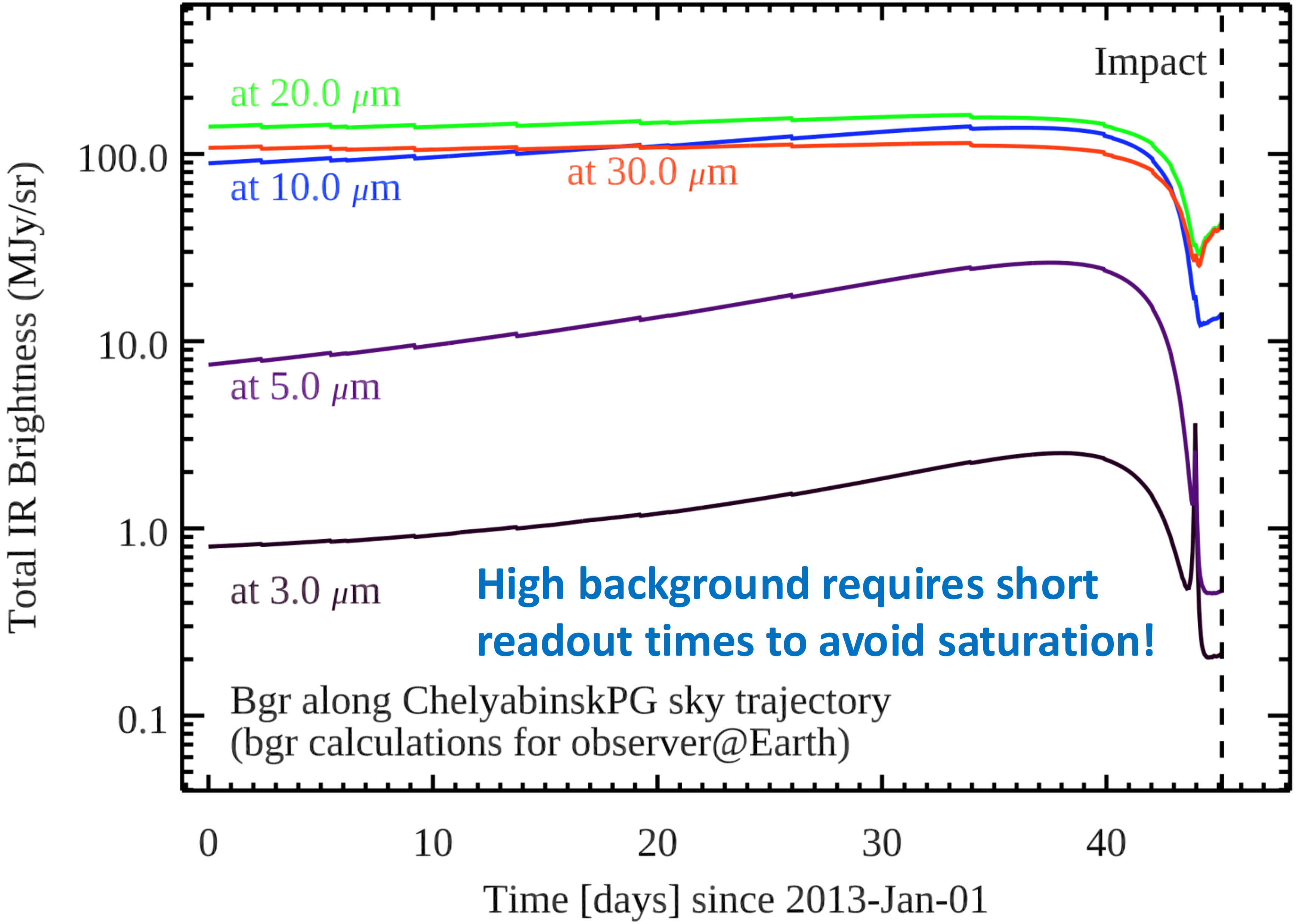

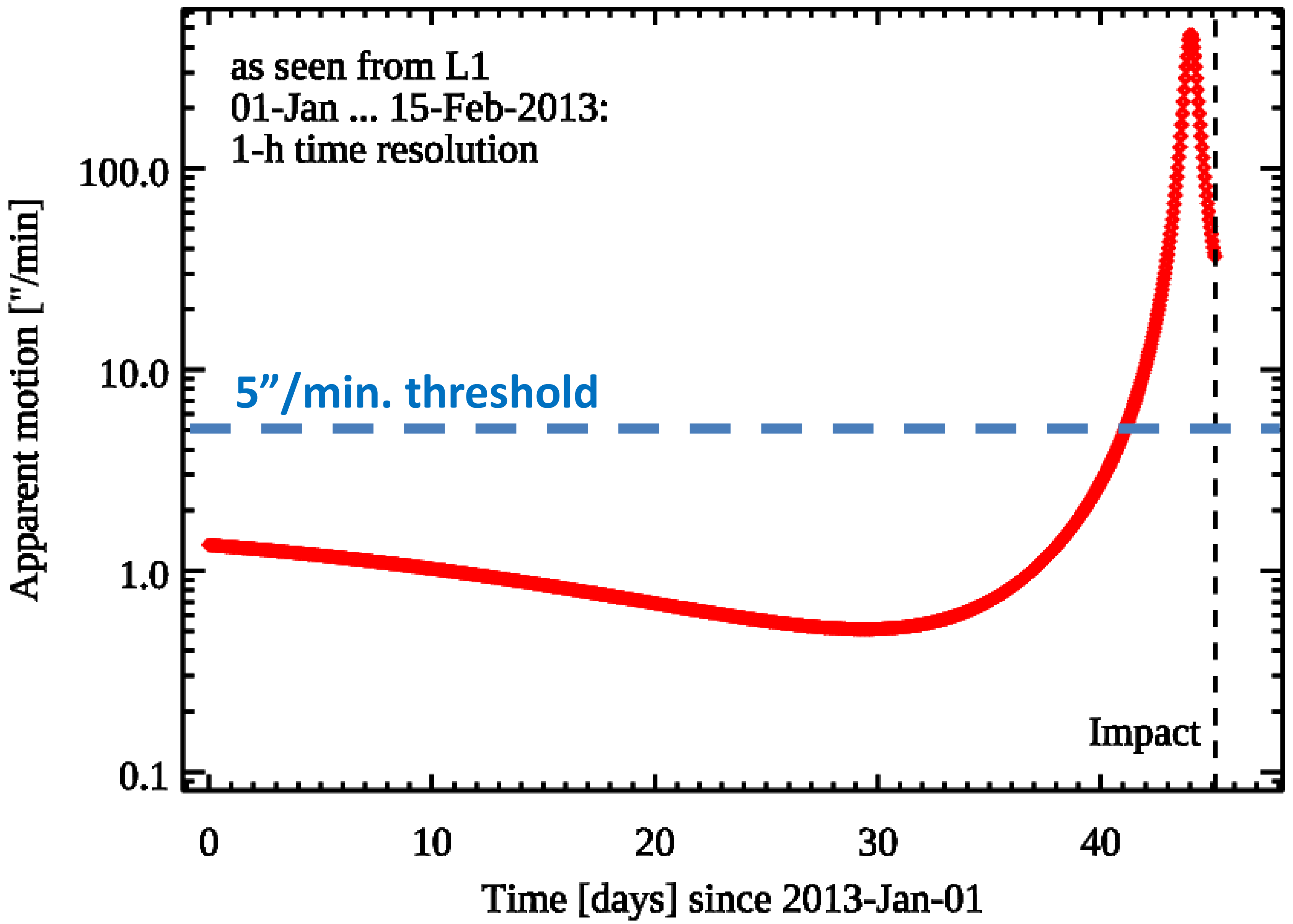
as seen from L1
01-Jan ... 15-Feb-2013:
1-h time resolution
5"/min. threshold
Impact
100.0
10.0
1.0
0.1
Apparent motion ["/min]
0
10
20
30
40
Time [days] since 2013-Jan-01

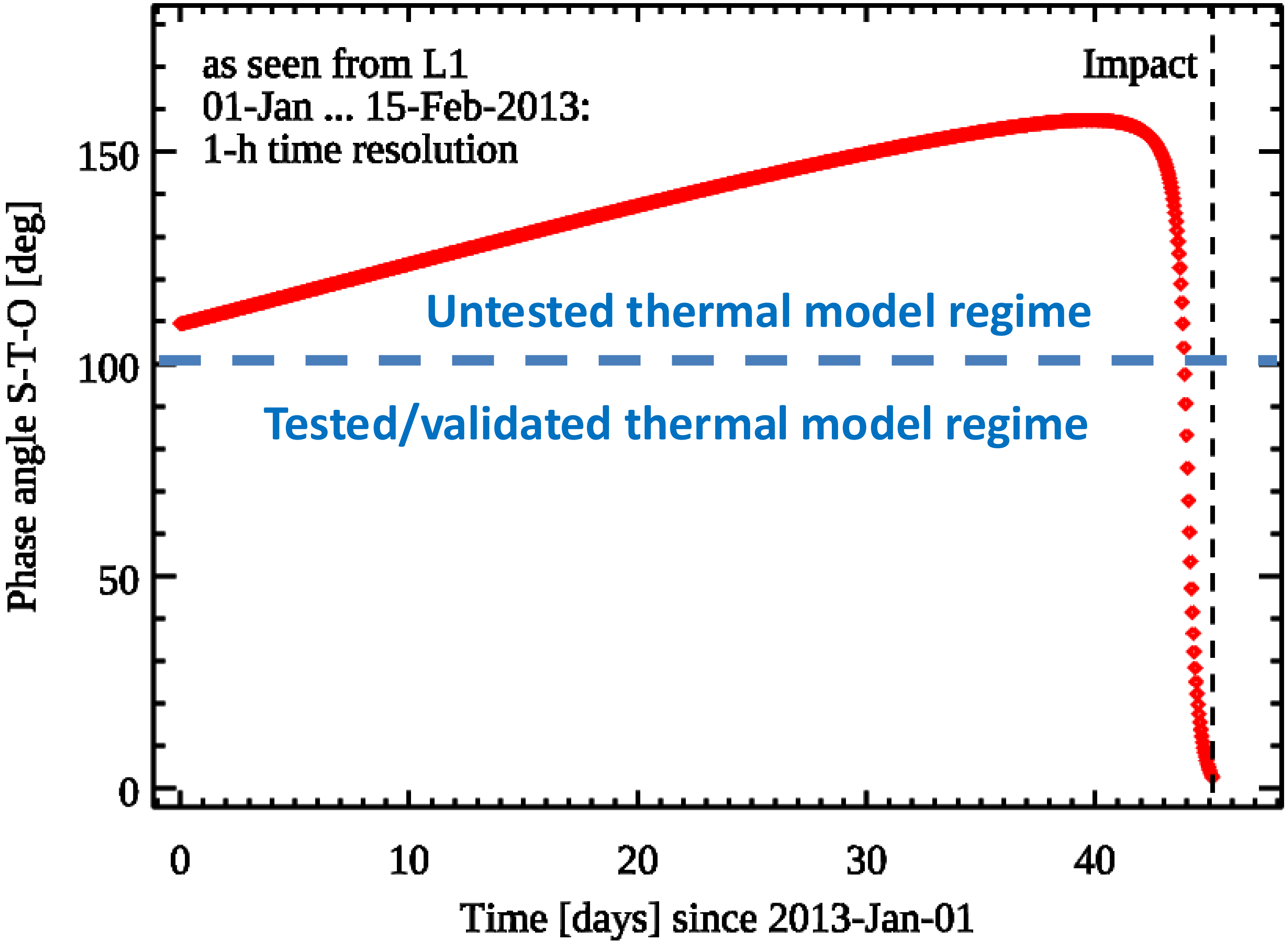

as seen from L1
01-Jan ... 15-Feb-2013:
1-h time resolution
Impact
Untested thermal model regime
Tested/validated thermal model regime
Phase angle S-T-O [deg]
0
50
100
150
0
10
20
30
40
Time [days] since 2013-Jan-01

Different model predictions at 8 μm

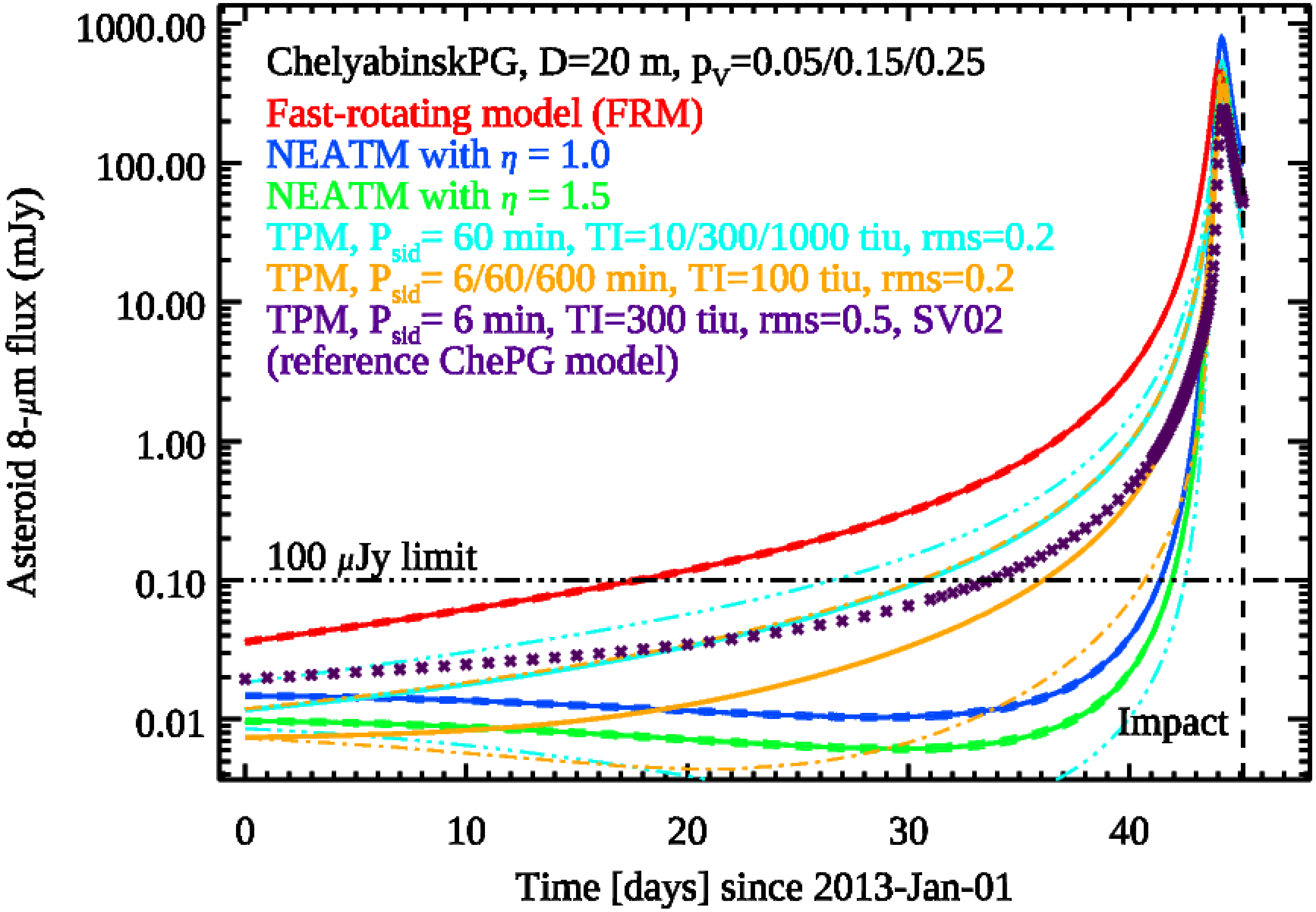

Pre-impact detection of Chelyabinsk-type objects in the thermal infrared

A pre-impact detection (and size estimate) of a Chelyabinsk-type object is possible:

- **with a 50 cm telescope, large FOV, passively cooled detector**
- **from L1, at 8-10 µm, 8-10 days before impact (while the object is still fainter than mag 30!)**
- **but requires observations down to 20° solar elongation, at very high background, produces high data rates and needs synthetic tracking techniques (to take advantage of full array-crossing times)!**
- **Large uncertainties in the predictions remain due to unknowns in the asteroid IR models!**

Difficulty to model IR emission of small asteroids at high phase angles

- The thermal model predictions for (small, fast-rotating?, monolithic?, porous?) NEOs is very difficult and uncertain, especially for high phase angles (> 90 °)
- There is clearly a lack of IR measurements of asteroids seen under large phase angles!
- NEOs below ~200 m in size are rotating faster (Pravec et al. 2008): → FRM?
- However, NEATM (with beaming parameters η in the range 1-1.5) seem to work for about 50 NEOs with sizes between ~8 to ~100 m (Mainzer et al. 2014): → NEATM?
- The Yarkovsky drift of a rapidly rotating small asteroid points to an unexpectedly low thermal inertia, indicative for a highly porous or cracked surface (Petkovic et al. 2021; Fenucci et al. 2023): → TPM?
- There is also the vector alignment of asteroid spins by thermal torques (YORP), see work by Vokrouhlicky et al. (2003): → TPM?
- Our baseline model: TPM with D= 20 m, p_V = 0.15, Γ=300 tiu, roughness rms = 0.5, P_{sid} = 6 min, β_{ecl} = +45 °, ε=0.9 (fluxes between NEATM with η=1.0 or 1.5 and FRM for wide phase angle ranges)

NEOSurveyor visibility zone:
$45^\circ \leq (\lambda - \lambda_\odot) \leq 125^\circ$
$-41.9^\circ \leq \beta_{ecl} \leq +41.9^\circ$

Detectability: about 1 day 16 h before impact
8 h on Feb-13 and 2 h on Feb-14

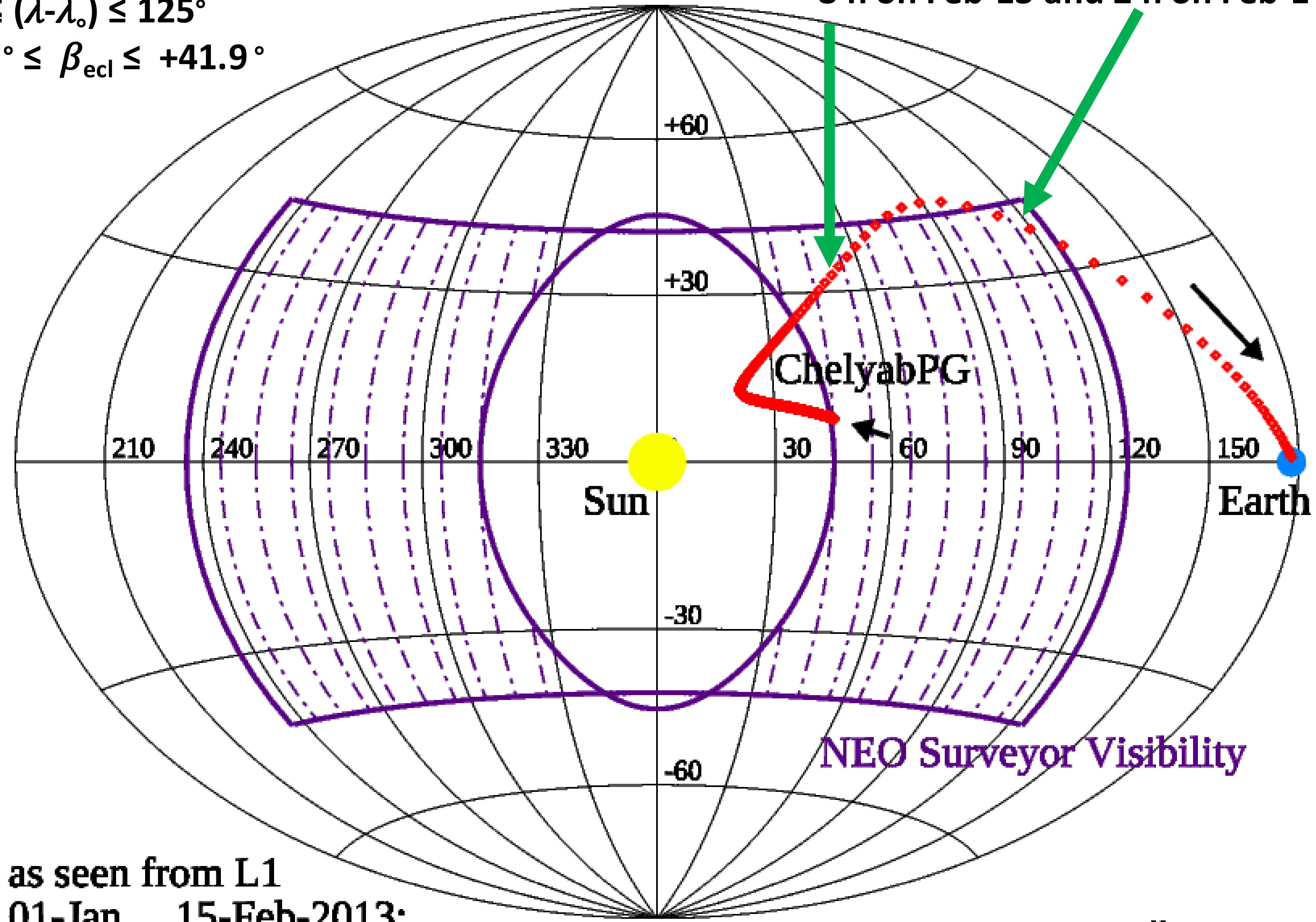

as seen from L1
01-Jan ... 15-Feb-2013:
1-h time resolution

Aitoff Projection
T.Mueller, Aug 24

NEOMIR visibility zone:
30° ≤ (S-O-T) ≤ 70°
[-70° ≤ β_{ecl} ≤ +70°]

Detectability: about 2 days 6 h before impact
for about 24 hours

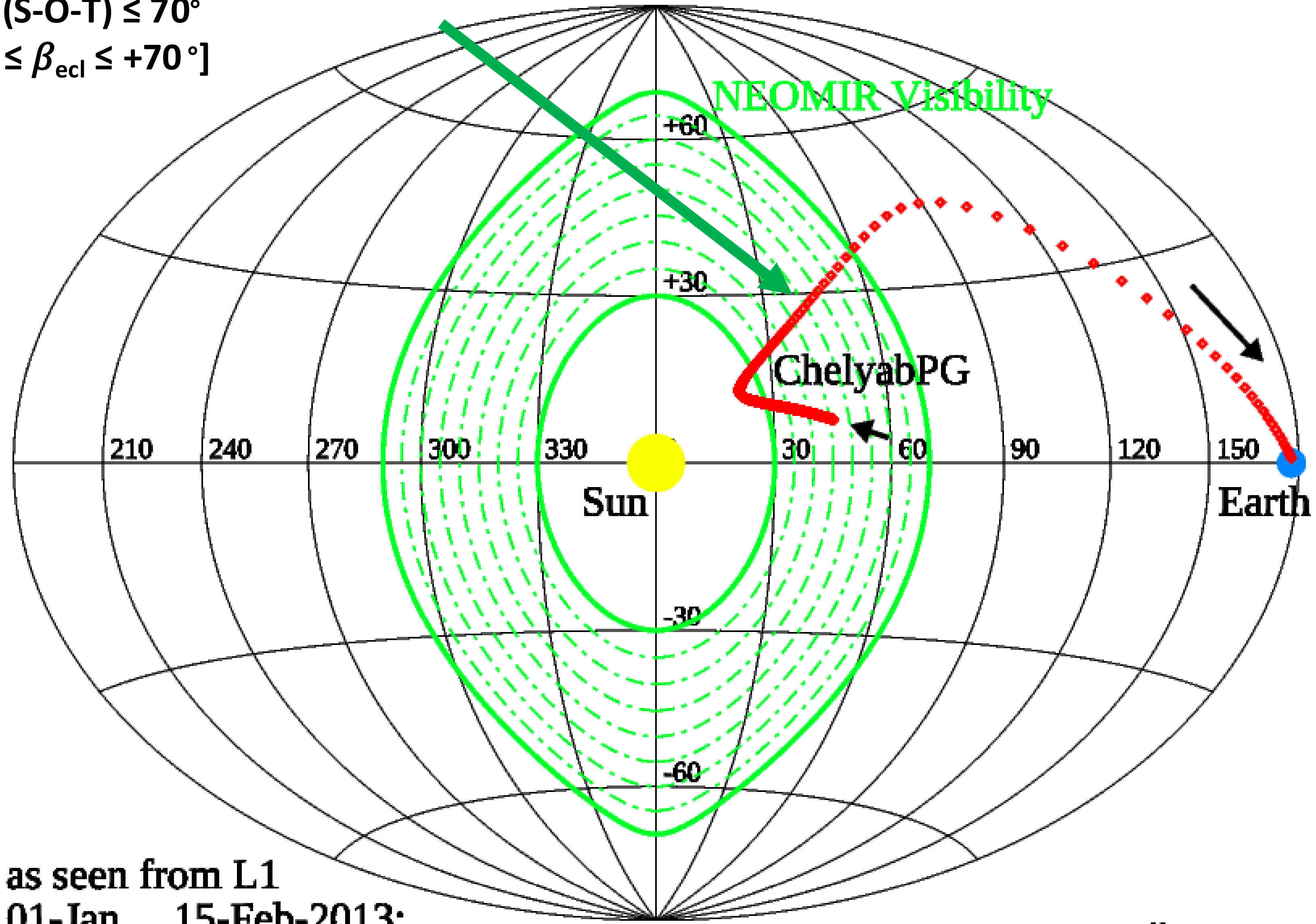

as seen from L1
01-Jan ... 15-Feb-2013:
1-h time resolution

Aitoff Projection
T.Mueller, Aug 24

Different model predictions at 8 μm